RSC Advances

REVIEW

View Article Online
View Journal | View Issue

Open Access Article. Published on 26 April 2022. Downloaded on 7/17/2025 7:12:56 PM.
This article is licensed under a Creative Commons Attribution-NonCommercial 3.0 Unported Licence.

Check for updates

Cite this: *RSC Adv.*, 2022, **12**, 12672

Recent advances in the application of magnetic bio-polymers as catalysts in multicomponent reactions

Zohreh Kheilkordi,[a] Ghodsi Mohammadi Ziarani,*[a] Fatemeh mohajer,[a] Alireza Badiei[b] and Mika Sillanpää[cde]

Magnetic nanoparticles have attracted significant attention due to their high surface area and superparamagnetic properties. Bio-polymers composed of polysaccharides including alginate, cellulose, glucose, dextrin, chitosan, and starch can be immobilized on magnetic nanoparticles. Bio-polymers can be obtained from natural sources, such as plants, tunicates, algae, and bacteria. Bio-polymers obtained from natural sources have attracted attention due to their various properties including efficient functional groups, non-toxicity, low cost, availability, and biocompatibility. According to the targets of "green chemistry", the application of bio-polymers is effective in reducing pollution. Furthermore, they are excellent agents for the functionalization of magnetic nanoparticles to yield nanomagnetic bio-polymers, which can be applied as recoverable and eco-friendly catalysts in multicomponent reactions.

Received 25th February 2022
Accepted 7th April 2022

DOI: 10.1039/d2ra01294d

rsc.li/rsc-advances

1. Introduction

Among the various magnetic nanoparticles, nano magnetic iron oxide (Fe_3O_4) is very important because of its low cost, easy synthesis, and high magnetic ability. Recently, magnetic nanoparticles have been extensively applied in various fields including drug delivery, sensing, water treatment, removal of heavy metals, and catalysis. However, they are unstable in alkaline and acidic media due to the easy oxidation of their surface area.[1–8] These drawbacks can be alleviated *via* the modification of Fe_3O_4 nanoparticles with materials such as silanes,[9,10] activated carbon,[11] and biocompatible polymers.[12,13] Another class of magnetic nanoparticles is ferrite magnetic nanomaterials and hexaferrite (M-type). Ferrite magnetic nanomaterials and hexaferrite have various applications including high chemical strength materials, home appliances, supercapacitors, loudspeakers, electromagnetic wave absorption, and permanent magnets.[14–18] Overall, due to the properties of ferrite magnetic nanomaterials and hexaferrite (M-type), they can be used for the adsorption of various metals ions, cationic and anionic dyes from wastewater.[19–23]

The design and synthesis of biocompatible magnetic nanoparticles are important subjects in green chemistry.[24] Bio-polymers including alginate, cellulose, glucose, dextrin, chitosan, and starch are known as polysaccharides, which are present in the carbohydrates in plants, animals, microbes, and algae (Fig. 1).[24] These bio-polymers have different properties such as biodegradable nature, biocompatibility, non-toxicity, availability, low cost, and heat resistantance.[25] They are excellent agents for the functionalization of magnetic nanoparticles to yield nanomagnetic bio-polymers, promoting their longevity, hardness, and strength. These composites have many applications such as drug delivery,[26–28] chemotherapy,[29,30] magnetic resonance imaging (MRI) agents,[31,32] solar cells,[33] chemical sensors,[34,35] catalysts,[36] water treatment,[37,38] and biomedical sensors.[39]

In comparison to conventional catalysts, heterogeneous magnetic bio-polymers have various advantages such as non-toxicity, easy separation, and eco-friendly nature. According to the functional groups on the magnetic nanoparticles, the catalysts can be grouped in various categories including, Lewis and Brønsted acids and bases.[40,41] In continuation of our research,[42–44] in this review, the importance of nanomagnetic bio-polymers is studied in multicomponent reactions. Multicomponent reactions (MCRs) are essential tools in medicinal and organic chemistry, which have various advantages including simplicity, easy workup, availability, and reduced generation of waste. Hence, the design and application of MCRs for the synthesis of organic compounds are highly important.[45–50]

---

[a] *Department of Chemistry, Faculty of Physics and Chemistry, Alzahra University, Tehran, Iran, 1993893979. E-mail: gmohammadi@alzahra.ac.ir; Fax: +98 2188613937; Tel: +98 2188613937*

[b] *School of Chemistry, College of Science, University of Tehran, Tehran, Iran*

[c] *Department of Chemical Engineering, School of Mining, Metallurgy and Chemical Engineering, University of Johannesburg, P. O. Box 17011, Doornfontein 2028, South Africa. E-mail: Mika.Sillanpaa@uef.fi*

[d] *Department of Applied Physics, Faculty of Science and Technology, Universiti Kebangsaan Malaysia, 43600 Bangi, Selangor, Malaysia*

[e] *International Research Centre of Nanotechnology for Himalayan Sustainability (IRCNHS), Shoolini University, Solan, 173212, Himachal Pradesh, India*

© 2022 The Author(s). Published by the Royal Society of Chemistry

Open Access Article. Published on 26 April 2022. Downloaded on 7/17/2025 7:12:56 PM.
This article is licensed under a Creative Commons Attribution-NonCommercial 3.0 Unported Licence.

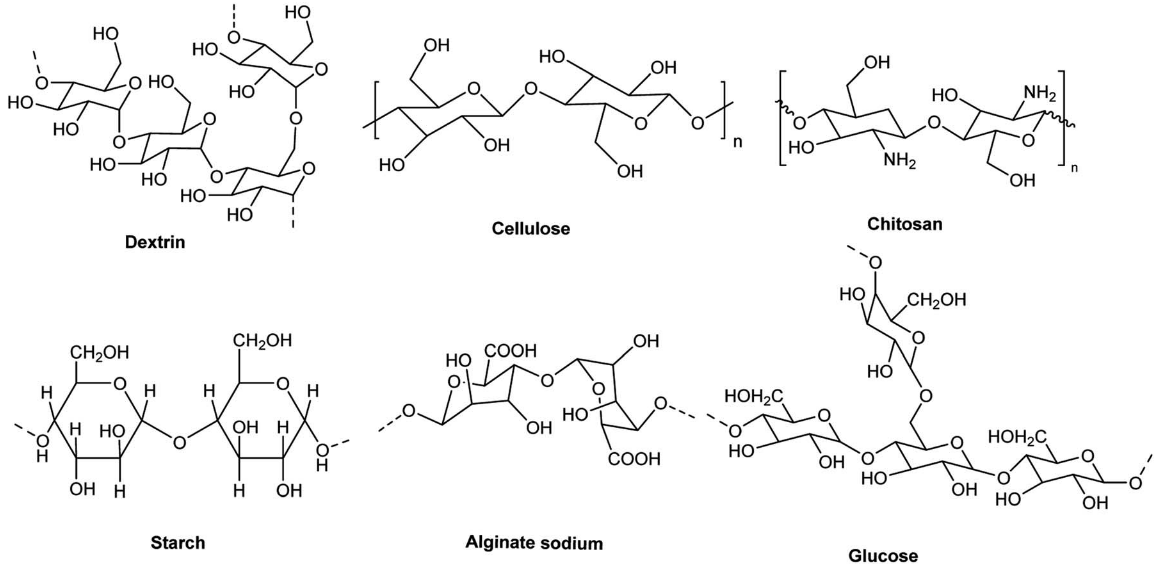

Fig. 1 Various bio-polymers.

2. Synthesis of various magnetic bio polymers

2.1. Magnetic bio-polymers based on cellulose

2.1.1. Synthesis and application of Fe_3O_4/cellulose/Co-MOF nanocomposite. Initially, Fe_3O_4 nanoparticles **4** were modified with cellulose **5** using urea **6**/NaOH **7** to provide Fe_3O_4/cellulose **8**, which was reacted with $Co(NO_3)_2 \cdot 6H_2O$ **9**, terephthalic acid **10**, and imidazole (IM) **11** in DMF to form Fe_3O_4/cellulose/Co-MOF nanocomposite **12** (Scheme 1).[51]

Fe_3O_4/cellulose/Co-MOF **12** has two sites including Lewis acidic sites (Co^{2+}) and basic sites (IM), which were used in the Knoevenagel condensation reaction of aromatic aldehydes **13** with malononitrile **14** under solvent-free conditions (Scheme 2). This catalyst was reused five times without a decrease its catalytic activity.[51]

2.1.2. Synthesis and application of Fe_3O_4@NCs/Sb(V). Initially, raw cotton was converted to nano-cellulose (NCs) **5** in the presence of NaOH **7**, NaClO **16**, and H_2SO_4 **17** at 80 °C. Then, Fe_3O_4 was functionalized with nano-cellulose (NCs) **5**, providing Fe_3O_4@NCs **8**. In the next step, $SbCl_5$ was mixed with the reaction mixture in chloroform to provide Fe_3O_4@NCs/Sb(V) **18** (Scheme 3).[52]

Fe_3O_4@NCs/Sb(V) was used as a Lewis acid for the activation of carbonyl groups, which was investigated in the synthesis of 4*H*-pyrimido[2,1-*b*]benzothiazoles **22** *via* the three-component reaction of aldehydes **19**, 2-aminobenzothiazole **20**, and ethylacetoacetate **21** under solvent-free conditions at 90 °C (Scheme 4). This catalyst was used five times without loss in its catalytic activity, which was compared with Fe_3O_4 with 39% yield in 3 h.[52]

2.1.3. Synthesis and application of Fe_3O_4@NFC@Co(II). Fe_3O_4 MNPs were synthesized *via* the reaction of $FeCl_3 \cdot 6H_2O$ and $FeSO_4 \cdot 7H_2O$ in the presence of NH_4OH solution at 80 °C under an N_2 atmosphere. The Fe_3O_4 nanoparticles were dispersed in H_2O, and then nanofiber cellulose (NFC) **24** was added to the reaction mixture at room temperature to obtain Fe_3O_4@NFC **25** precipitate, which was reacted with an ethanolic solution of cobalt(II) acetate to form Fe_3O_4@NFC@Co(II) **26** (Scheme 5).[53]

Its catalytic activity was useful for the synthesis of 4*H*-pyrans *via* the multicomponent reaction of aldehydes, ethylacetoacetate, and malononitrile in H_2O (Scheme 6).[53]

Also, the catalytic activity of **26** was tested for the synthesis of pyranopyrazole derivatives **29** *via* the four-component reaction of hydrazine hydrate **28**, ethyl acetoacetate **21**, benzaldehyde **19**, and malononitrile **14** in H_2O (Scheme 7). The metal ions on the catalyst surface act as Lewis acids, which were activated by the malononitrile and carbonyl groups. Also, the catalyst was used five times in the model reaction without a reduction in activity.[53]

2.1.4. Synthesis and application of cellulose@pumice. Initially, the microcrystalline cellulose was mixed with a solution of NaOH **7** and urea **6** in H_2O, and then was cooled in an ice bath at 8 °C to form a gel solution, which was mixed with pumice powder **32** and stirred for 24 h to obtain cellulose@pumice **33** (Scheme 8).[54]

Cellulose@pumice as an acidic catalyst activated carbonyl groups in the synthesis of 2,4,5-triarylimidazoles **36** through the reaction of benzaldehyde **19** and ammonium acetate **35** in EtOH under ultrasonic irradiation (Scheme 9). In the reusability test, this catalyst was used ten times without a reduction in activity.[54]

2.1.5. The synthesis and application of (Fe_3O_4@NFC@NSalophCu)CO_2H. Nanofiber cellulose **37** was functionalized with Fe_3O_4 *via* the sol–gel method to give Fe_3O_4@NFC nanoparticles **39**, which were functionalized with (3-aminopropyl)triethoxysilane (APTES) **40** to obtain Fe_3O_4@NFC@APTES **41**. The reaction of salicylaldehyde **42**, paraformaldehyde **43**, and HCl solution under reflux conditions provided 5-chloromethyl salicylaldehyde **44**, which was reacted with 3,5-diaminobenzoic acid **45** in CH_2Cl_2 at room temperature to give the Schiff base 3,5-bis(((*E*)-5-(chloromethyl)-2-

Open Access Article. Published on 26 April 2022. Downloaded on 7/17/2025 7:12:56 PM. This article is licensed under a Creative Commons Attribution-NonCommercial 3.0 Unported Licence.

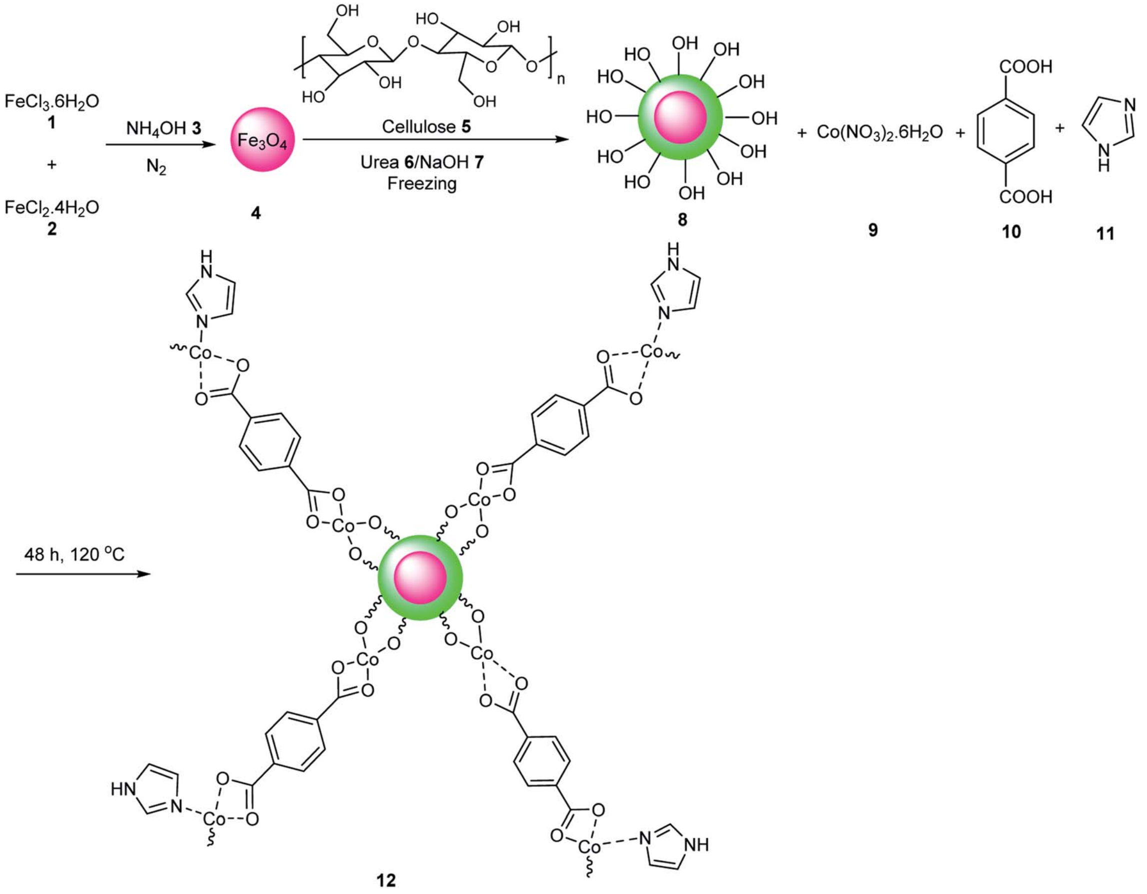

Scheme 1 Synthesis of Fe_3O_4/cellulose/Co-MOF nanocomposite **12**.

hydroxybenzylidene)amino) benzoic acid ((5-Cl-Saloph)CO_2H) **46**, followed by reaction with copper acetate in EtOH at room temperature to obtain complex [(5-Cl-Saloph)Cu(II)]CO_2H **47**. Finally, the reaction of [(5-Cl-Saloph)Cu(II)]CO_2H complex **47** and Fe_3O_4@NFC@APTES **41** at 70 °C for 24 h gave (Fe_3O_4@NFC@NSalophCu)CO_2H **48** (Scheme 10).[55]

(Fe_3O_4@NFC@NSalophCu)CO_2H **48** was tested in the synthesis of 5-substituted-1*H*-tetrazole **51** *via* the multicomponent reaction of various aldehydes **19**, hydroxylamine **49**, and sodium azide **50** (Scheme 11), and also in the synthesis of 1-substituted-1H-tetrazoles **54** *via* the multicomponent reaction of aniline **52**, triethyl orthoformate **53**, and sodium azide **50** (Scheme 12). This catalyst was used in the click reaction four times without a decrease in its activity. In this catalyst, copper metal plays a vital role in the click reactions.[55]

2.1.6. Synthesis and application of Fe_3O_4@NFC@NNSM-Mn(III). Fe_3O_4 nanoparticles were functionalized with NFC nanospheres to prepare Fe_3O_4@NFC **39**, which was dispersed in toluene, and then 3-chloropropyl-trimethoxy silane **55** was added to the reaction mixture under N_2 gas and reflux conditions to obtain Fe_3O_4@NFC–Cl **56**, followed by reaction with *o*-phenylenediamine **54** in CH_2Cl_2 under reflux conditions to give Fe_3O_4@NFC@NN **57**. Then, 5-(chloromethyl)-2-hydroxy benzaldehyde **58** was reacted with Fe_3O_4@NFC@NN **57** to form Fe_3O_4@NFC@NNS **59**, which was complexed with $Mn(OAc)_3 \cdot 2H_2O$ **60** in EtOH to prepare Fe_3O_4@NFC@NNS-Mn **61**, followed by reaction with melamine **62** in the presence of triethylamine in MeOH to generate Fe_3O_4@NFC@NNSM-Mn(III) **63** (Scheme 13).[56]

The activity of Fe_3O_4@NFC@NNSM-Mn(III) **63** was tested for the synthesis of xanthenes **65** *via* the pseudo-three-component reaction of aldehydes **19** and dimedone **64** in EtOH at 45 °C (Scheme 14). The manganese metal on the surface of Fe_3O_4@NFC@NNSM-Mn(III) acts as a Lewis acid to activate the carbonyl groups. This catalyst was used five times without a decrease in its activity.[56]

2.1.7. Synthesis and application of Fe_3O_4@NFC@ONSM-Ni(II). Initially, Fe_3O_4@NFC **39** was functionalized with 3-chloropropyl-trimethoxy silane **55** to obtain Fe_3O_4@NFC@CPTMS **56**. Subsequently, 2-hydroxy 4-chloromethyl benzaldehyde **44** was prepared *via* the reaction of salicylaldehyde **42**, paraformaldehyde **43**, and HCl 37% in the presence of H_2SO_4 as a catalyst at 70 °C for 20 h. In the next step, the Schiff base ligand was synthesized *via* the reaction of 2-aminophenol **66** and 5-chloromethylsalicyaldehyde **67** in dichloromethane at 40 °C for 3 h. Then, Fe_3O_4@NFC@ONS **68** was obtained through the reaction of 4-(chloromethyl)-2-(((2-hydroxyphenyl)imino) methyl) phenol **67** and Fe_3O_4@NFC@CPTMS **68** in the presence of triethylamine in acetonitrile under reflux conditions. In the next step, Fe_3O_4@NFC@ONS **68** was reacted with $Ni(OAc)_2$

© 2022 The Author(s). Published by the Royal Society of Chemistry

Open Access Article. Published on 26 April 2022. Downloaded on 7/17/2025 7:12:56 PM.
This article is licensed under a Creative Commons Attribution-NonCommercial 3.0 Unported Licence.

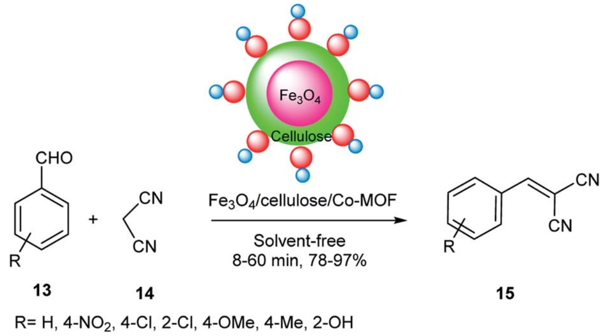

Scheme 2 Knoevenagel condensation in the presence of Fe_3O_4/cellulose/Co-MOF **12**.

in EtOH at room temperature for 12 h to obtain Fe_3O_4@NFC@ONS-Ni(II) **69**. Finally, Fe_3O_4@NFC@ONSM-Ni(II) **70** was synthesized as a nanocatalyst *via* the reaction of Fe_3O_4@NFC@ONS-Ni(II) **69** and melamine **62** in the presence of triethylamine in the MeOH under reflux conditions and N_2 gas for 12 h (Scheme 15).[57]

This catalyst was used in the synthesis of polyhydroquinolines **72** through the Hantzsch reaction among benzaldehydes **19**, dimedone **64**, ethyl acetoacetate **21**, and ammonium acetate **71** (Scheme 16).[57]

Also, Bagherzade *et al.* applied this catalyst in the synthesis of 1,4-dihydropyridine **72** *via* the multicomponent reaction of aldehydes **19**, ethyl acetoacetate **21**, and ammonium acetate **71** (Scheme 17). The carbonyl groups in the multi-component reaction were activated in the presence of nickel metal on the surface of Fe_3O_4@NFC@ONSM-Ni(II) as a Lewis acid. Also, this catalyst was tested 6 times without loss in its activity.[57]

2.1.8. Synthesis and application of cell-LA-TEA$^+$/Fe_3O_4. Initially, cellulose **5** was reacted with tosyl chloride **74** in the presence of Et_3N to form cell-tosyl **75**, which was reacted with lactic acid **76** to produce cell-LA **77**, followed by reaction with triethanolamine **78** to prepare cell-LA-TEA$^+$ **79**. Finally, cell-LA-TEA$^+$ **79** was magnetized *via* the reaction of $FeCl_3 \cdot 6H_2O$, $FeCl_2 \cdot 4H_2O$, and ammonium solution in aqueous media to form cell-LA-TEA$^+$/Fe_3O_4 **80** (Scheme 18).[58]

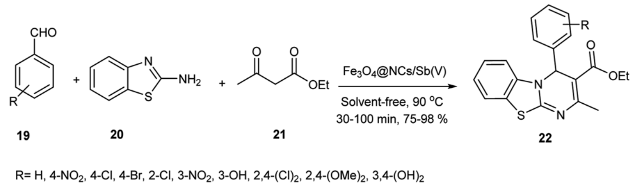

Scheme 4 Synthesis of 4*H*-pyrimido[2,1-*b*]benzothiazole derivatives **22**.

Cell-LA-TEA$^+$/Fe_3O_4 was used as a catalyst for the regioselective synthesis of pyrazolo quinolones **82** *via* the three-component reaction of dimedone **64**, 5-amino pyrazolone **81**, and aromatic aldehydes **19** in EtOH/H_2O under ultrasonic irradiation (Scheme 19). The catalyst was used with high stability in 7 cycles without loss in its activity.[58]

2.1.9. Synthesis and application of Fe_3O_4@nano-cellulose-OPO_3H. Initially, nano-cellulose **5** was prepared from cotton. Then, Fe_3O_4@nano-cellulose (Fe_3O_4@NCs) **8** was obtained through the reaction of nano-cellulose solution in acetic acid with $FeCl_3 \cdot 6HO_2$, $FeCl_2 \cdot 4H_2O$, and ammonium hydroxide at 80 °C. Finally, Fe_3O_4@NCs were immobilized with P_4O_{10} at room temperature under grinding conditions to produce Fe_3O_4@NCS-PA **83** (Scheme 20).[59]

2,3-Dihydroquinazolin-4(1*H*)-ones **85** were prepared *via* the condensation reaction of 2-aminobenzamide **84** and aldehydes **19** in the presence of Fe_3O_4@NCS-PA **83** as a Brønsted acid in H_2O: EtOH under reflux conditions (Scheme 21). The main

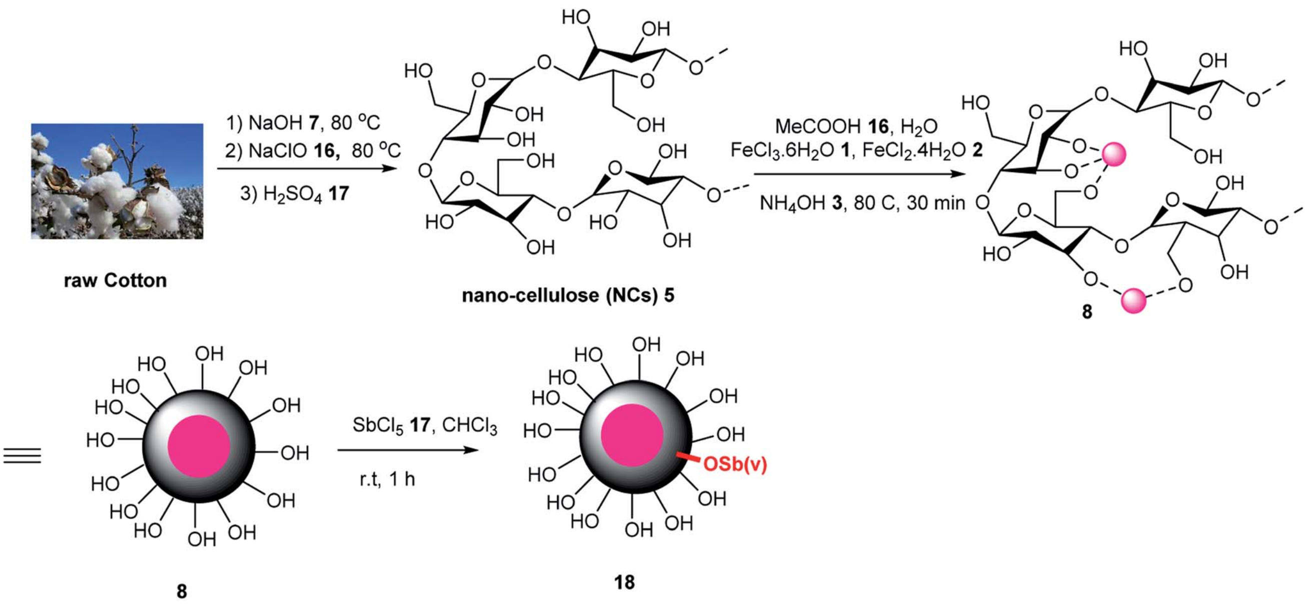

Scheme 3 Synthesis of Fe_3O_4@NCs/Sb(v).

Open Access Article. Published on 26 April 2022. Downloaded on 7/17/2025 7:12:56 PM. This article is licensed under a Creative Commons Attribution-NonCommercial 3.0 Unported Licence.

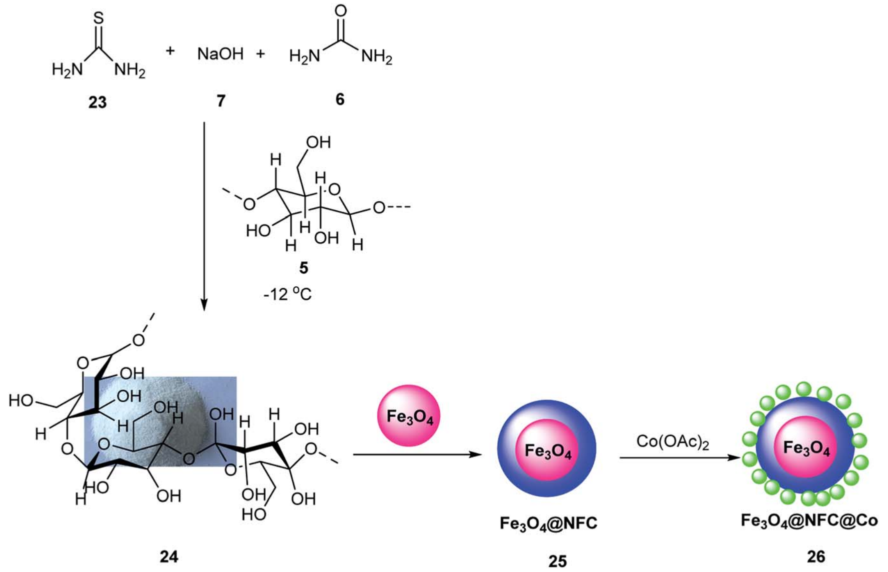

Scheme 5 Synthesis of Fe_3O_4@NFC@Co(II) **26**.

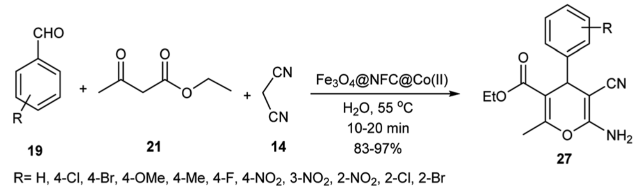

Scheme 6 Synthesis of 4*H*-pyrans **27** in the presence of Fe_3O_4@NFC@Co(II).

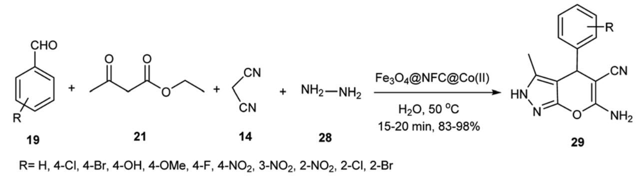

Scheme 7 Synthesis of pyranopyrazole derivatives **29** using Fe_3O_4@NFC@Co(II).

advantages of this method are its excellent yields, simple workup, and eco-friendly catalyst. This reaction was accomplished in H_2O: EtOH under reflux conditions in the presence of Fe_3O_4 with 60% yield; however, Fe_3O_4@NCS-PA performed better than Fe_3O_4 in this reaction.[59]

2.1.10. Synthesis and application of Fe_3O_4@NCs/Cu(II). Fe_3O_4 was functionalized with nano-cellulose **5** to obtain

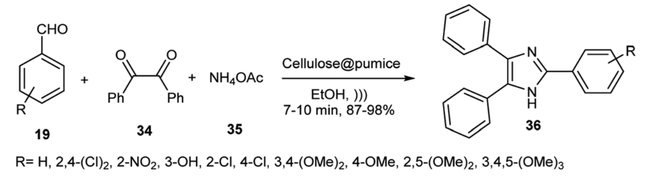

Scheme 9 Synthesis of 2,4,5-triarylimidazoles derivatives **36**.

Fe_3O_4@NCs **8**, which was added to NaOH solution to give Fe_3O_4@NCs **8**, followed by reaction with $CuCl_2$ to provide Fe_3O_4@NCs/Cu(II) **86** (Scheme 22).[60]

Fe_3O_4@NCs/Cu(II) as a Lewis acid activated the carbonyl groups of the starting materials by copper metal in the synthesis of indenopyrido[2,3-*d*]pyrimidines **89** through the three-component reaction of 6-amino-2-(methylthio)pyrimidin-4(3*H*)-one **88**, 1,3-indanedione **87** and aldehydes **19** in EtOH (Scheme 23). The activity of the catalyst was preserved after four runs.[60]

2.1.11. Synthesis and application of Fe_3O_4@nano-cellulose/Cu(II). The reaction of nano-cellulose **5**, $FeCl_3 \cdot 6H_2O$, $FeCl_2 \cdot 4H_2O$, and NH_4OH at 80 °C gave Fe_3O_4@nano-cellulose **8**, which was reacted with $CuCl_2$ using sodium hydroxide at room temperature to obtain Fe_3O_4@nano-cellulose/Cu(II) **90** (Scheme 24).[61]

Cu(II) in Fe_3O_4@nanocellulose/Cu(II), as a Lewis acid, activated the carbonyl groups in the three-component reaction of

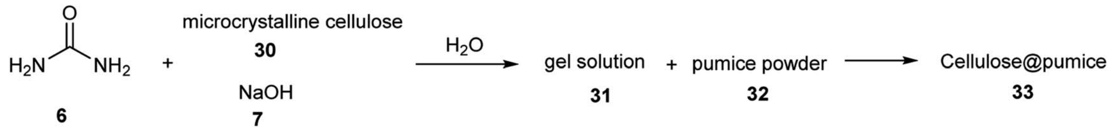

Scheme 8 Synthesis of cellulose@pumice **33**.

© 2022 The Author(s). Published by the Royal Society of Chemistry

Open Access Article. Published on 26 April 2022. Downloaded on 7/17/2025 7:12:56 PM.
This article is licensed under a Creative Commons Attribution-NonCommercial 3.0 Unported Licence.

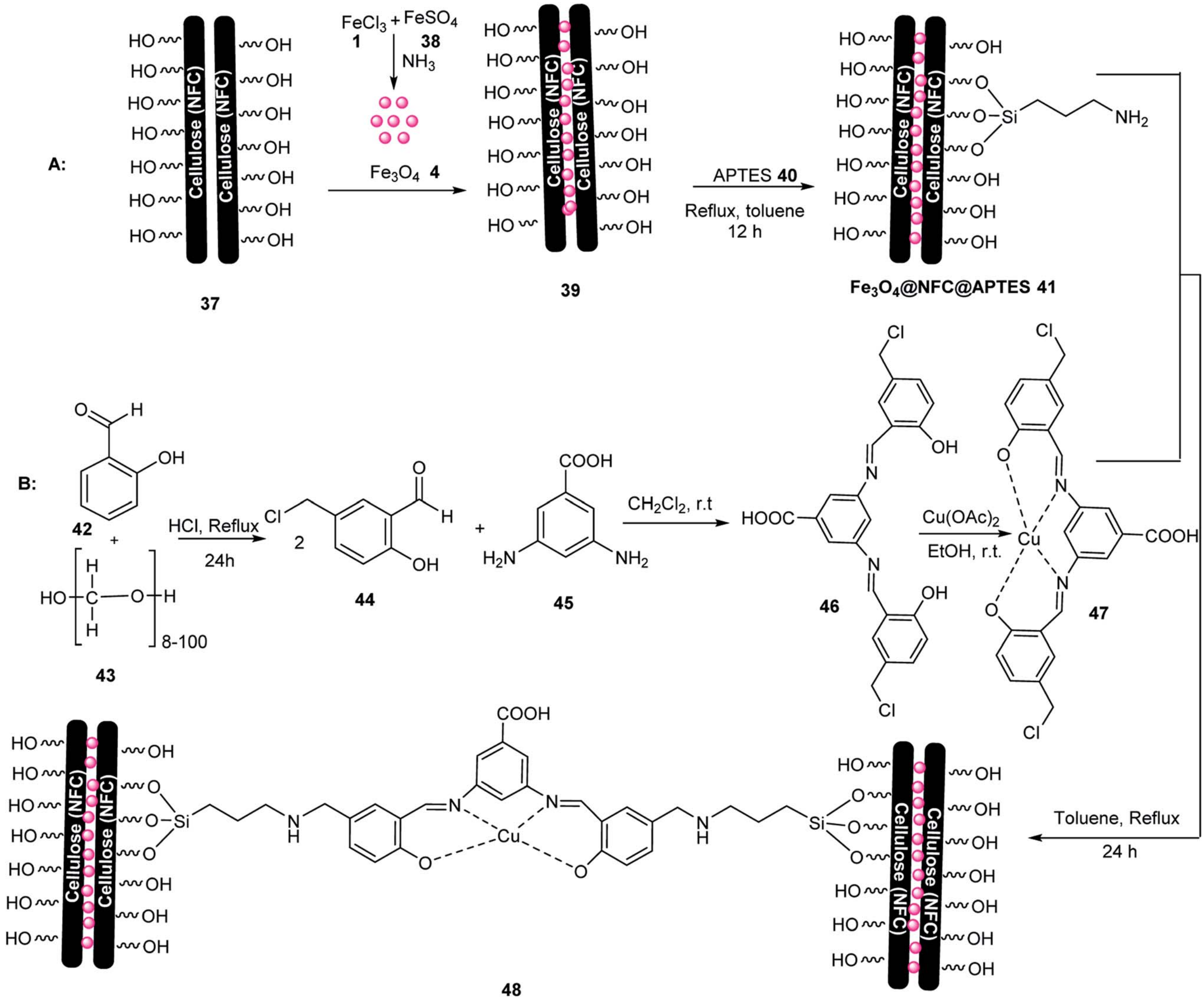

Scheme 10 Synthesis of $(Fe_3O_4@NFC@NSalophCu)CO_2H$.

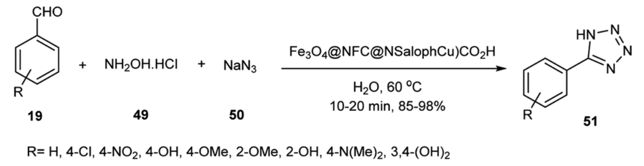

Scheme 11 Synthesis of 5-substituted-1*H*-tetrazole **47** using $(Fe_3O_4@NFC@NSalophCu)CO_2H$.

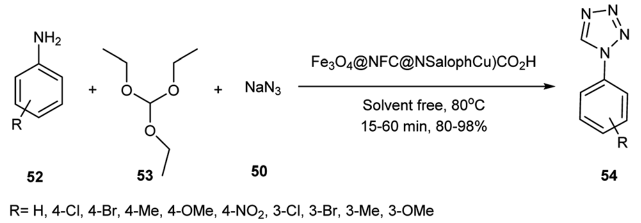

Scheme 12 Synthesis of 1-substituted-1*H*-tetrazoles using $(Fe_3O_4@NFC@NSalophCu)CO_2H$.

aromatic aldehydes **19**, 2-aminobenzothiazole **20**, and ethyl acetoacetate **21** for the synthesis of 4*H*-pyrimido[2,1-*b*]benzothiazoles **22** (Scheme 25). The catalyst activity of Fe_3O_4@nanocellulose/Cu(II) was preserved after four runs. The yield of this reaction in the presence of Fe_3O_4 as a catalyst after 3 h was reported to be about 37%. Therefore, Fe_3O_4@nano-cellulose/Cu(II) is more active than Fe_3O_4.[61]

2.1.12. Synthesis and application of Fe_3O_4@NFC-ImSalophCu(II). Initially, imidazole **11** was treated with 3-chloropropyl-trimethoxy silane **55** in toluene to produce imidazole-propyl-trimethoxy silane **91**, which was immobilized on Fe_3O_4@NFC **39** using Et_3N as a catalyst in dry toluene to give Fe_3O_4@NFC-Im **92**. The reaction of salicylaldehyde **42** and paraformaldehyde **43** in the presence of HCl/H_2SO_4 gave 5-(chloromethyl)-2-hydroxybenz aldehyde **44**, which was reacted with 1,2-phenylenediamine **93** in dichloromethane under reflux

Open Access Article. Published on 26 April 2022. Downloaded on 7/17/2025 7:12:56 PM.
This article is licensed under a Creative Commons Attribution-NonCommercial 3.0 Unported Licence.

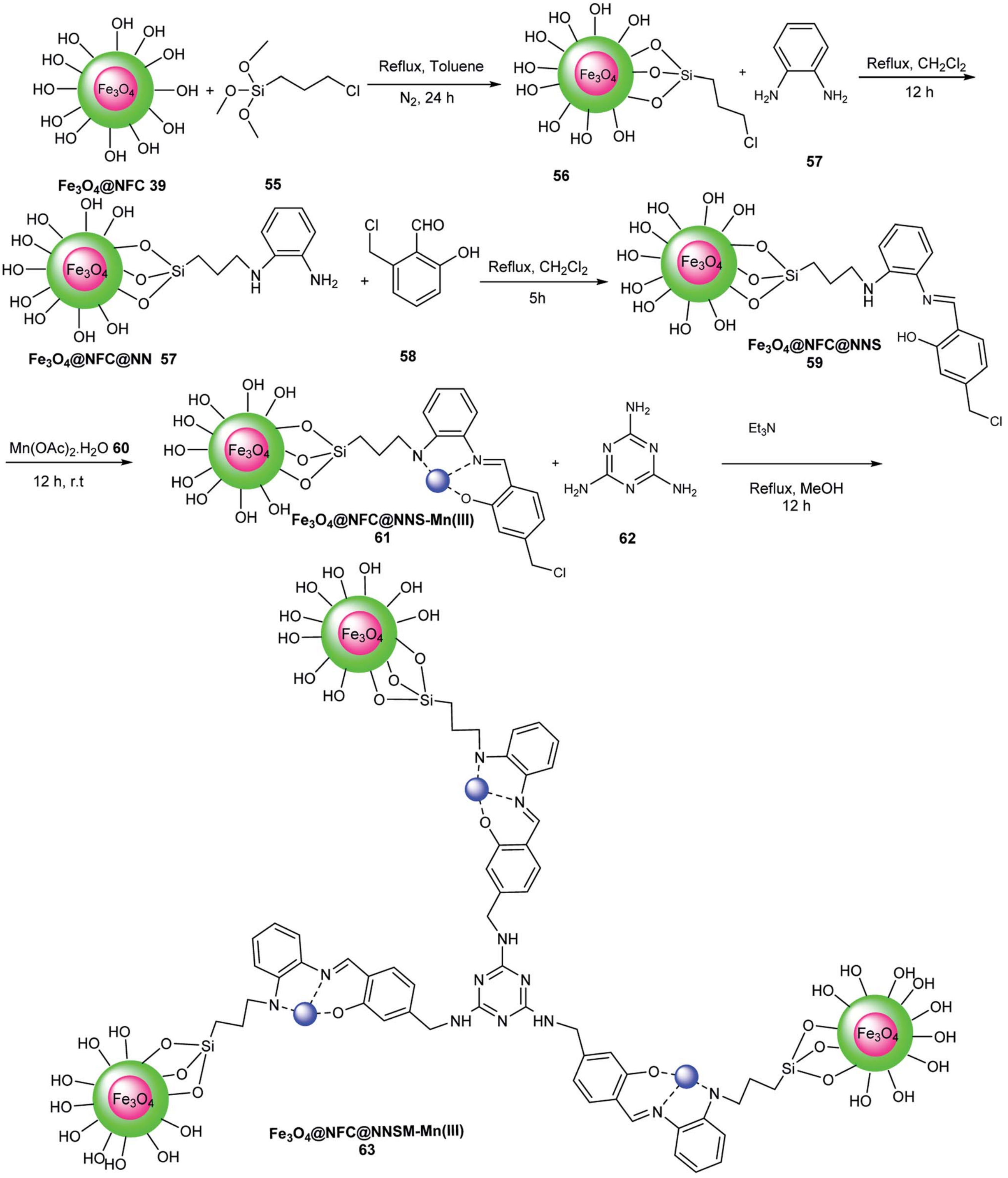

Scheme 13 Synthesis of Fe_3O_4@NFC@NNSM-Mn(III).

conditions to produce *N*,*N*-bis(5-chloromethylsalicylidene)-1,2-phenylenediamine **94**, followed by reaction with $Cu(OAc)_2$ in EtOH at room temperature to prepare 5-Cl-Salophen-Cu(II) **95**. Finally, Fe_3O_4@NFC-ImSalophCu(II) **96** was synthesized *via* the reaction of Fe_3O_4@NFC-Im **92** and 5-Cl-Salophen-Cu(II) **95** in toluene under reflux conditions (Scheme 26).[62]

The copper of Fe_3O_4@NFC-ImSalophCu **96** was applied in the click reaction of phenacyl bromides **97**, sodium azide **90**,

Open Access Article. Published on 26 April 2022. Downloaded on 7/17/2025 7:12:56 PM.
This article is licensed under a Creative Commons Attribution-NonCommercial 3.0 Unported Licence.

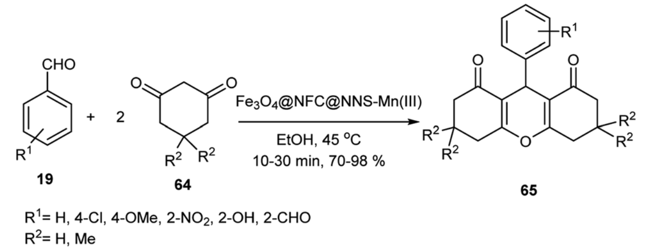

Scheme 14 Synthesis of xanthene derivatives **65** in the presence of Fe_3O_4@NFC@NNSM-Mn(III).

and alkynes **98** in H_2O to synthesize 1,2,3-triazoles **99** (Scheme 27). The reusability of this catalyst was tested in the click reaction four times without loss in its activity.[62]

2.1.13. Synthesis and application of Fe_3O_4@walnut shell/Cu(II). Nanomagnetic Fe_3O_4@walnut shell/Cu(II) was prepared by Mirjalili's research group. Nanomagnetic Fe_3O_4@walnut shell/Cu(II) **100** was prepared *via* the reaction of dried powdered walnut shell with NaOH, hypochlorite solution, and sulfuric acid aqueous to afford a nano walnut shell, followed by reaction with CH_3COOH, $FeCl_3\cdot 6H_2O$ **1**, $FeCl_2\cdot 4H_2O_2$, and NH_4OH to generate nanomagnetic Fe_3O_4@walnut shell **8**, which was modified by $CuCl_2\cdot 2H_2O$/NaOH to produce nanomagnetic Fe_3O_4@walnut shell/Cu(II) **100** (Scheme 28).[63]

Its catalytic activity was explored using 2-aryl/alkyl-2,3-dihydro-1*H*-naphtho[1,2-*e*][1,3]oxazines **102** or **104** or **106** *via* the *pseudo*-three-component reaction of β-naphthol **101** or α-naphthol **103** or phenol derivatives **105,** formaldehyde **52**, and various amines **43** (Scheme 29). The catalytic activity of nano-Fe_3O_4@walnut shell/Cu did not decrease after five-times use. The copper metal on the nano-Fe_3O_4@walnut shell/Cu(II) increased the reaction rate *via* interaction with the carbonyl group of the starting materials.[63]

2.2. Magnetic bio-polymers based on dextrin

2.2.1. Synthesis and application of magnetic dextrin nanocomposite. Dextrin **107** is a water-soluble polysaccharide obtained *via* the hydrolysis of starch and glycogen. Magnetic dextrin nanocomposite **108** was prepared *via* the addition of dextrin **107** to a solution of $FeCl_3\cdot 6H_2O$, $FeCl_2\cdot 4H_2O$, and ammonium hydroxide at 90 °C under an N_2 atmosphere *via* the co-precipitation method (Scheme 30).[64]

The magnetic dextrin was tested as a catalyst in the synthesis of polyhydroquinolines *via* four-component reactions of aromatic aldehydes **19**, ethyl acetoacetate **21**, dimedone **61**, ammonium acetate **71** in EtOH under reflux conditions (Scheme 31). The yield of the products did not decrease after five runs. This reaction was performed in the presence of dextrin in ethanol in 28% yield, and thus magnetic dextrin is better than dextrin to catalyze this reaction.[64]

2.2.2. Synthesis and application of magnetized dextrin. Magnetized dextrin **72** was obtained *via* the reaction of $FeCl_3\cdot 6H_2O$, $FeCl_2\cdot 4H_2O$, dextrin **71**, and NH_4OH in H_2O at 90 °C under a nitrogen atmosphere (Scheme 32).[65]

Maleki *et al.* studied the catalytic activity of magnetized dextrin **29** for the synthesis of dihydropyrano[2,3-*c*]pyrazoles **29** through the reaction of hydrazine hydrate **28**, ethyl acetoacetate **21**, aromatic aldehydes **19**, and malononitrile **14** under reflux conditions in EtOH (Scheme 33). This catalyst was used for five runs without a decrease in its catalytic activity.[65]

2.2.3. Synthesis and application of FND-Ti(IV). Fe_3O_4@nano-dextrin **108** was prepared through the reaction of nano-dextrin **107**, $FeCl_3\cdot 6H_2O$, $FeCl_2\cdot 4H_2O$, and ammonia solution in H_2O at 80 °C. Fe_3O_4@nano-dextrin **108** was coated with $TiCl_4$ in CH_2Cl_2 to prepare FND-Ti(IV) **109** (Scheme 34).[66]

Its catalytic activity as a Lewis acid was investigated in the synthesis of 2,3-dihydroquinazolin-4(1*H*)-ones **85** *via* the condensation reaction of 2-aminobenzamide **84** and aldehydes **19** under mild conditions (Scheme 35). This catalyst was used five times without loss in its catalytic activity.[66]

2.3. Magnetic bio-polymers based on starch

2.3.1. Synthesis and application of magnetic Ag/Fe_3O_4@starch nanocatalyst. To aqueous starch solution **110**, citric acid **111** and sodium hypophosphite **112** were added and refluxed to give the precipitate crude product, which was crushed and dried to give cross-linked starch **113**, followed by dissolving in H_2O to produce gelatinized starch **114**. The obtained gelatinized starch was reacted with $FeCl_3\cdot 6H_2O$, and $FeSO_4\cdot 7H_2O$ in H_2O at room temperature, and then mixed with NH_3 dropwise to give the Fe_3O_4@starch nanocatalyst, which was treated with $AgNO_3$ (aq) to generate the magnetic Ag/Fe_3O_4@starch **115** nanocatalyst (Scheme 36).[67]

The catalytic activity of Ag/Fe_3O_4@starch as Lewis acid **115** was evaluated in the one-pot reaction of benzaldehydes **19**, malononitrile **14**, and dimedone **64** in EtOH for the synthesis of 4*H*-pyran **116** (Scheme 37). Also, the magnetic nanocatalyst was reused five times with no loss in its activities.[67]

2.3.2. Synthesis and application of magnetic $CuFe_2O_4$@starch. To obtain $CuFe_2O_4$@starch **122**, $Cu(NO_3)_2$ **117** was reacted with $Fe(NO_3)_3$ **118** using sodium hydroxide in H_2O to give $CuFe_2O_4$ nanoparticles **121**, followed by reaction with starch to obtain $CuFe_2O_4$@starch **122**. Its catalytic activity was tested in the synthesis of 4*H*-chromene **125** or **126** *via* the three-component reaction of various aldehydes **19**, malononitrile **14**, 2-hydroxy-1,4-naphthoquinone **123**, or 4-hydroxycoumarin **124** (Scheme 38).[68]

In another attempt, 2-amino-5-oxo-5,6,7,8-tetrahydro-4*H*-benzo[*b*]pyrans **27** or **116** were synthesized *via* the reaction of aldehydes **19**, malononitrile **14**, and enolizable C–H-activated acidic compounds, including dimedone **64** and ethyl acetoacetate **21**, in the presence of $CuFe_2O_4$@starch **122** as a Lewis acid in EtOH. The reaction rate for aldehydes with electron-withdrawing groups was faster than that with electron-donating groups (Scheme 39 and 40), respectively. This catalyst was used in six runs without a decrease in its activity.[68]

2.3.3. Synthesis and application of magnetic starch/SPION@SO_3H. Superparamagnetic iron oxide nanoparticles (SPION) **127** were synthesized *via* the reaction of Fe^{2+}, Fe^{3+}, and ammonia in aqueous media. Then, SPION **127** was coated with

Open Access Article. Published on 26 April 2022. Downloaded on 7/17/2025 7:12:56 PM.
This article is licensed under a Creative Commons Attribution-NonCommercial 3.0 Unported Licence.

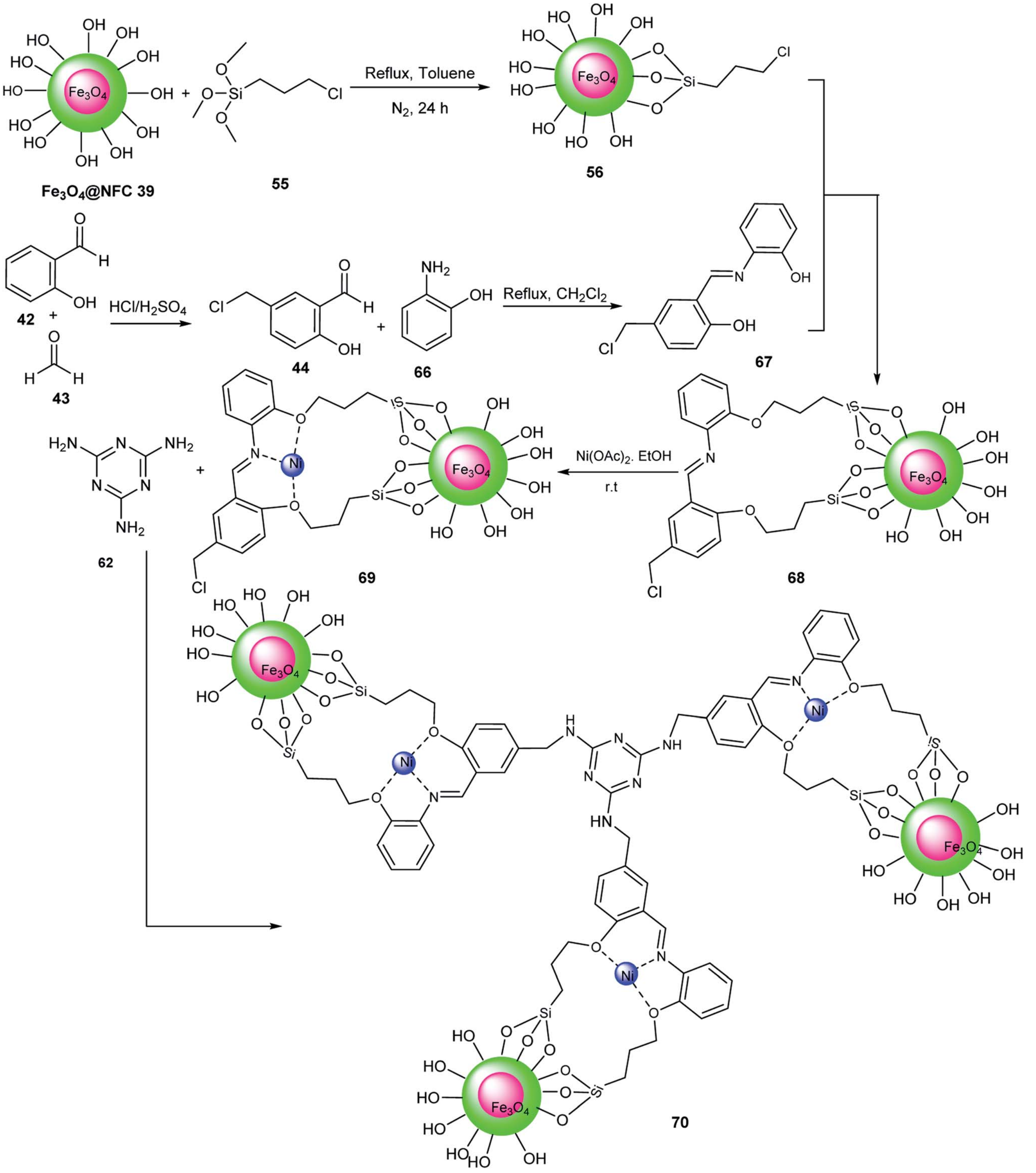

Scheme 15 Synthesis of Fe_3O_4@NFC@ONSM-Ni(II).

tetraethyl orthosilicate (TEOS) to give SPION@SiO_2 **128**, which was reacted with starch **110** to give magnetic starch, followed by reaction with allyltrimethoxysilane **130** to prepare allyl-functionalized magnetic starch **131**. Finally, starch/SPION@SO_3H **133** was synthesized *via* the polymerization of allyl-functionalized magnetic starch **131** and 4-styrenesulfonic acid **132** (Scheme 41).[69]

Starch/SPION@SO_3H **133** as a Brønsted acid (SO_3H) activated the carbonyl groups in the multicomponent reaction of 4-hydroxycoumarin **124**, benzaldehydes **19**, dimedone **64**, and

Open Access Article. Published on 26 April 2022. Downloaded on 7/17/2025 7:12:56 PM.
This article is licensed under a Creative Commons Attribution-NonCommercial 3.0 Unported Licence.

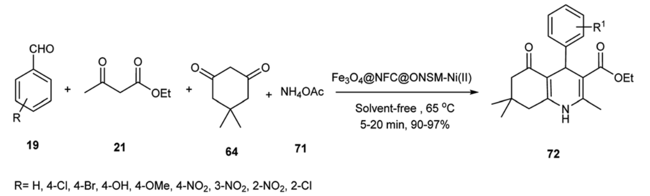

Scheme 16 Synthesis of polyhydroquinolines **72** in the presence of Fe_3O_4@NFC@ONSM(II).

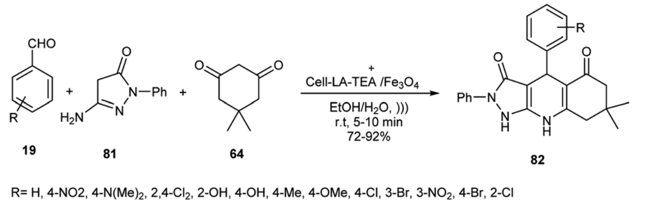

Scheme 19 Synthesis of pyrazolo quinolones **82** in the presence of Cell-LA-TEA^+/Fe_3O_4.

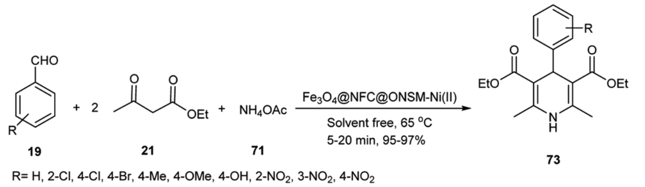

Scheme 17 Synthesis of 1,4-dihydropyridine **73** in the presence of Fe_3O_4@NFC@ONSM-Ni(II).

ammonium acetate **71** in the synthesis of chromeno[4,3-*b*]quinoline-6,8(9*H*)-dione derivatives **134** (Scheme 42). This catalyst was applied ten times without any loss in its activity.[69]

2.3.4. Synthesis and application of magnetic Fe_3O_4@GOTfOH/Ag/St-PEG-AcA. Initially, through the Hummers' method, graphite **135** was treated with H_2SO_4, $KMnO_4$, and H_2O to give GO **136**, which was treated with $FeCl_3$, $FeCl_2$, and ammonium solution at 80 °C to achieve Fe_3O_4@GO **137**, followed by reaction with trifluoro methanesulfonic acid in CH_2CH_2 to give Fe_3O_4@GOTfOH **138.** In the next step, starch **139** was dissolved in water at 80 °C. Subsequently, *N*,*N*-methylene acrylene acrylamide (MBA) **140** was dissolved in water. Then, the above-mentioned two mixtures were mixed to obtain a homogeneous viscous mixture. Then, a certain amount of acrylic acid **141** and PEG-poly **142** was added to the reaction mixture. Then, ammonium persulfate (APS) **143** solution was added to the reaction mixture until a hydrogel was obtained. The above-mentioned homogeneous solution, AgNP **144** colloidal solution and Fe_3O_4@GOTfOH **138** were mixed to obtain Fe_3O_4@GOTfOH/Ag/St-PEG-AcA **146** (Scheme 43).[70]

The catalytic activity of Fe_3O_4@GOTfOH/Ag/St-PEG-AcA **146** was examined in the synthesis of 2,4,6-triarylpyridines **137** through the pseudo-three-component reaction of aryl aldehydes **19**, acetophenone **147** and ammonium acetate **71** (Scheme 44). According to the catalyst structure, the carbonyl groups were activated *via* interaction with the Brønsted acid site and Lewis acid of Fe^{3+}. Also, the catalytic activity of **146** did not decrease after 10 runs.[70]

2.3.5. Synthesis and application of magnetic γ-Fe_2O_3@starch-*n*-butyl SO_3H. Fe_3O_4 nanoparticles **4** were synthesized *via* the reaction of $FeCl_2 \cdot 4H_2O$ **2** and $FeCl_3 \cdot 6H_2O$ **1** and NH_4OH solution in H_2O an under argon atmosphere at room

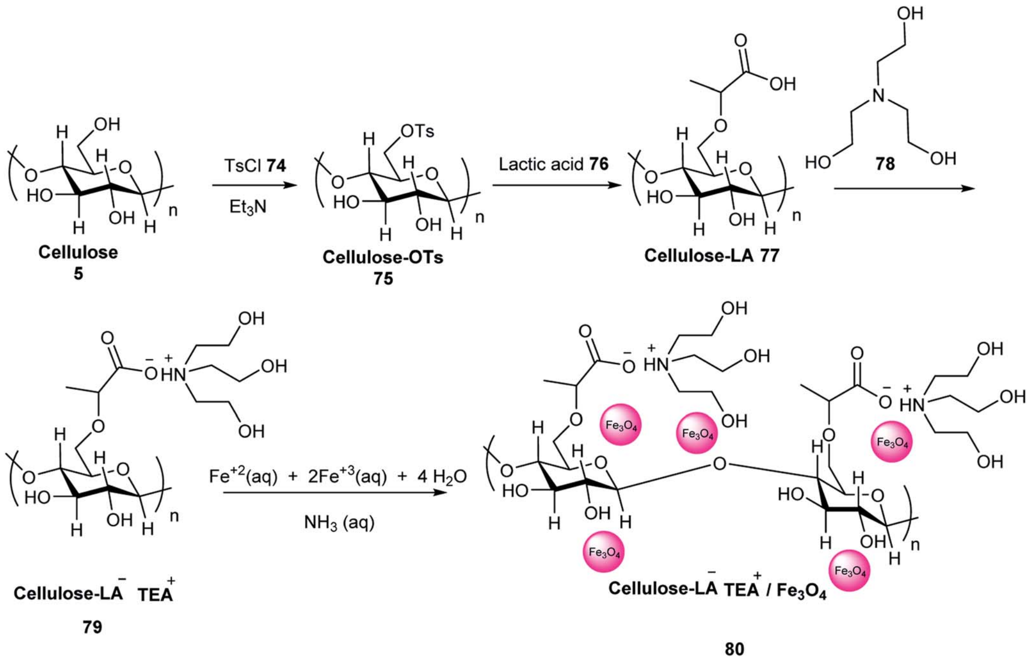

Scheme 18 Synthesis of Cell-LA-TEA^+/Fe_3O_4.

Open Access Article. Published on 26 April 2022. Downloaded on 7/17/2025 7:12:56 PM.
This article is licensed under a Creative Commons Attribution-NonCommercial 3.0 Unported Licence.

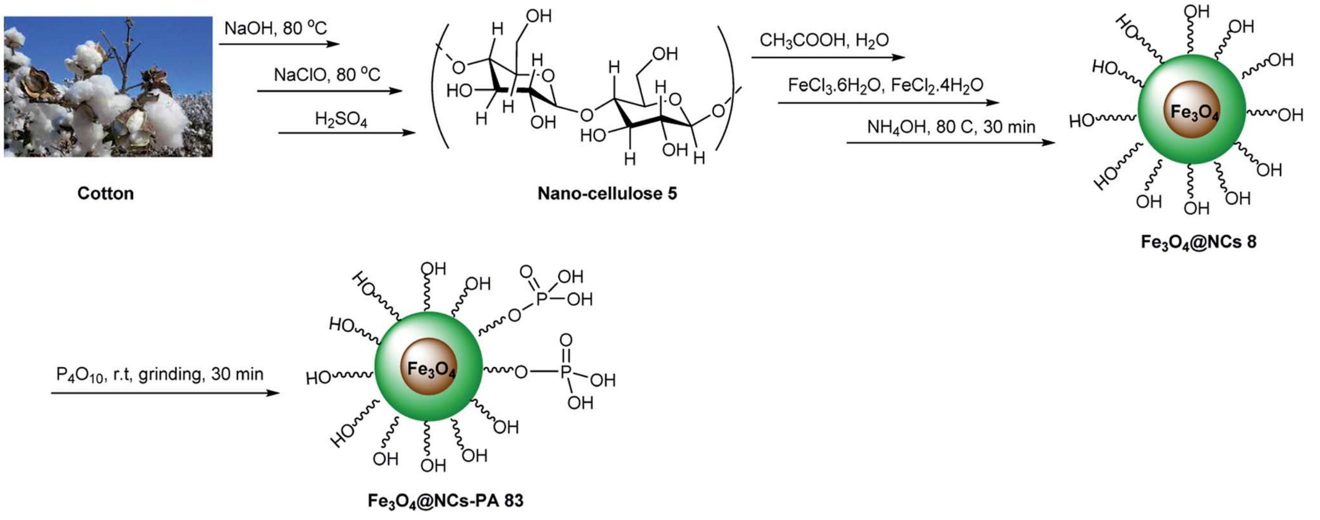

Scheme 20 Synthesis of Fe_3O_4@NCS-PA.

temperature. Then, γ-Fe_2O_3 was synthesized using Fe_3O_4 at 250 °C. In the next step, γ-Fe_2O_3 was coated with starch at room temperature to obtain γ-Fe_2O_3@starch **150**, followed by reaction with 1,4-butane sultone **151** in dry toluene under reflux conditions to produce γ-Fe_2O_3@starch-*n*-butylSO_3H **152** nanoparticles (Scheme 45).[71]

γ-Fe_2O_3@starch-*n*-butylSO_3H **152** as Brønsted acid activated the carbonyl groups in the multicomponent reactions of

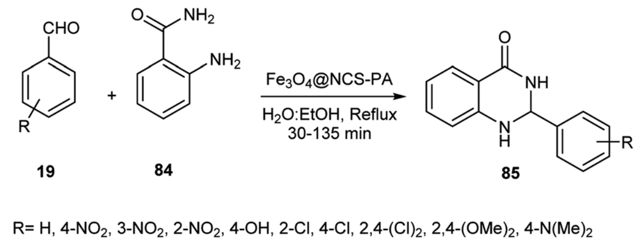

Scheme 21 Synthesis of 2,3-dihydroquinazolin-4(1*H*)-ones.

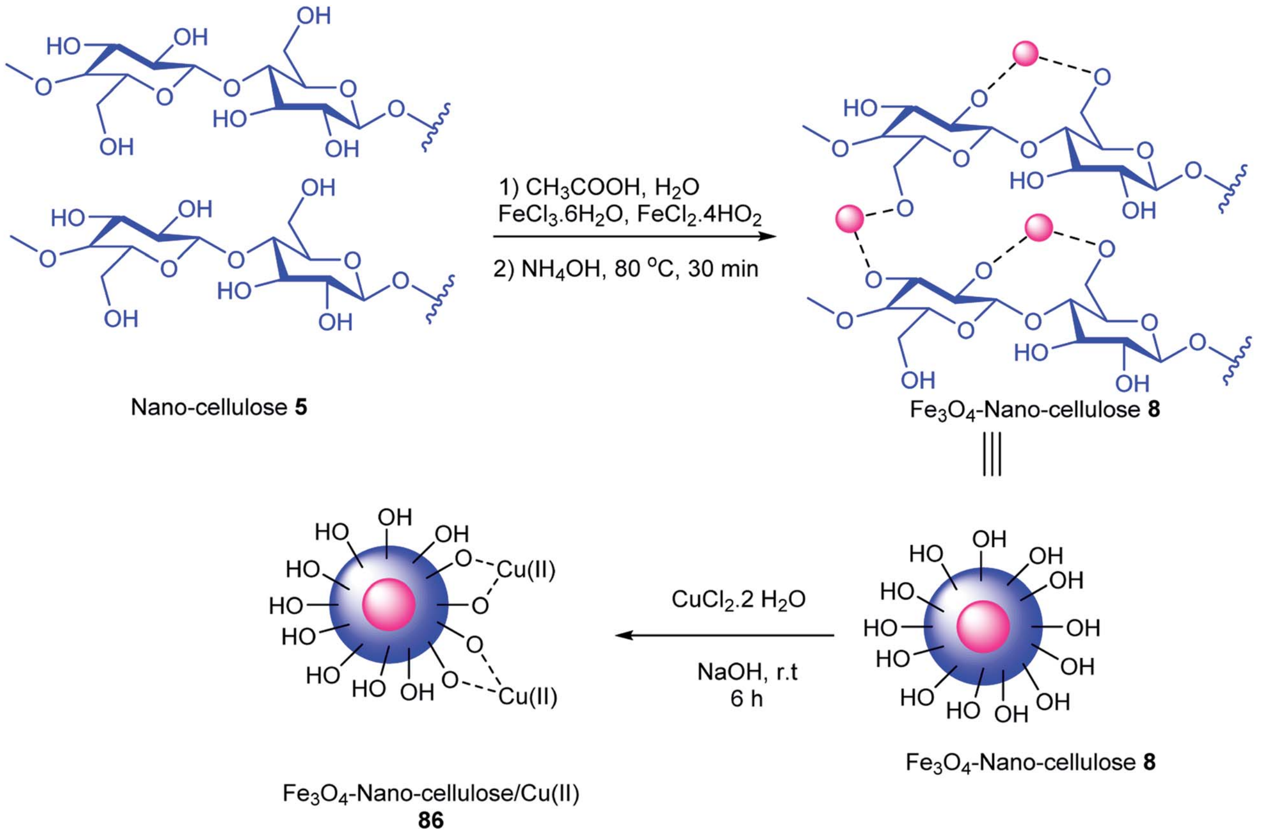

Scheme 22 Synthesis of Fe_3O_4@NCs/Cu(II) 86.

© 2022 The Author(s). Published by the Royal Society of Chemistry

Open Access Article. Published on 26 April 2022. Downloaded on 7/17/2025 7:12:56 PM.
This article is licensed under a Creative Commons Attribution-NonCommercial 3.0 Unported Licence.

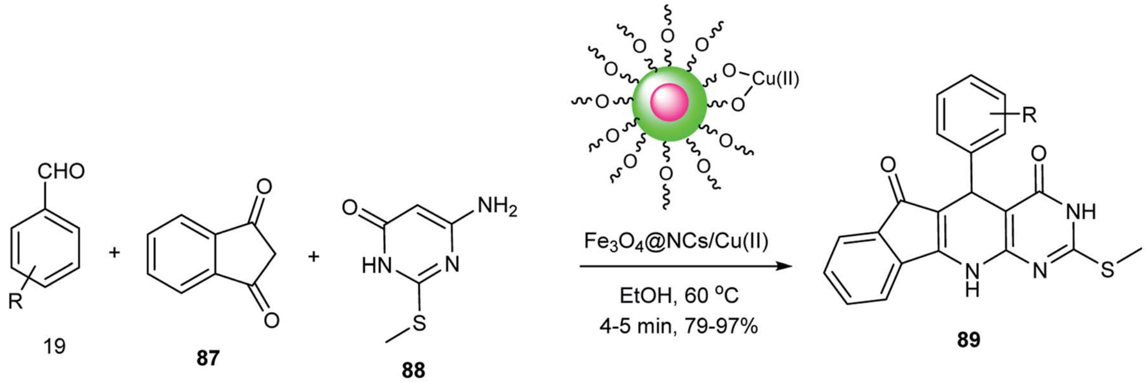

R= 4-Cl, 4-Br, 4-F, 2-Br, 2-Cl, 2-NO$_2$, 2,4-(Cl)$_2$, 2-OH, 4-Me, 4-OMe, 3,4-(OMe)$_2$, 4-OH-3-(OMe), 3-NO$_2$, 3-OH

Scheme 23 Synthesis of indenopyrido [2,3-*d*] pyrimidines in the presence of Fe_3O_4@NCs/Cu(II).

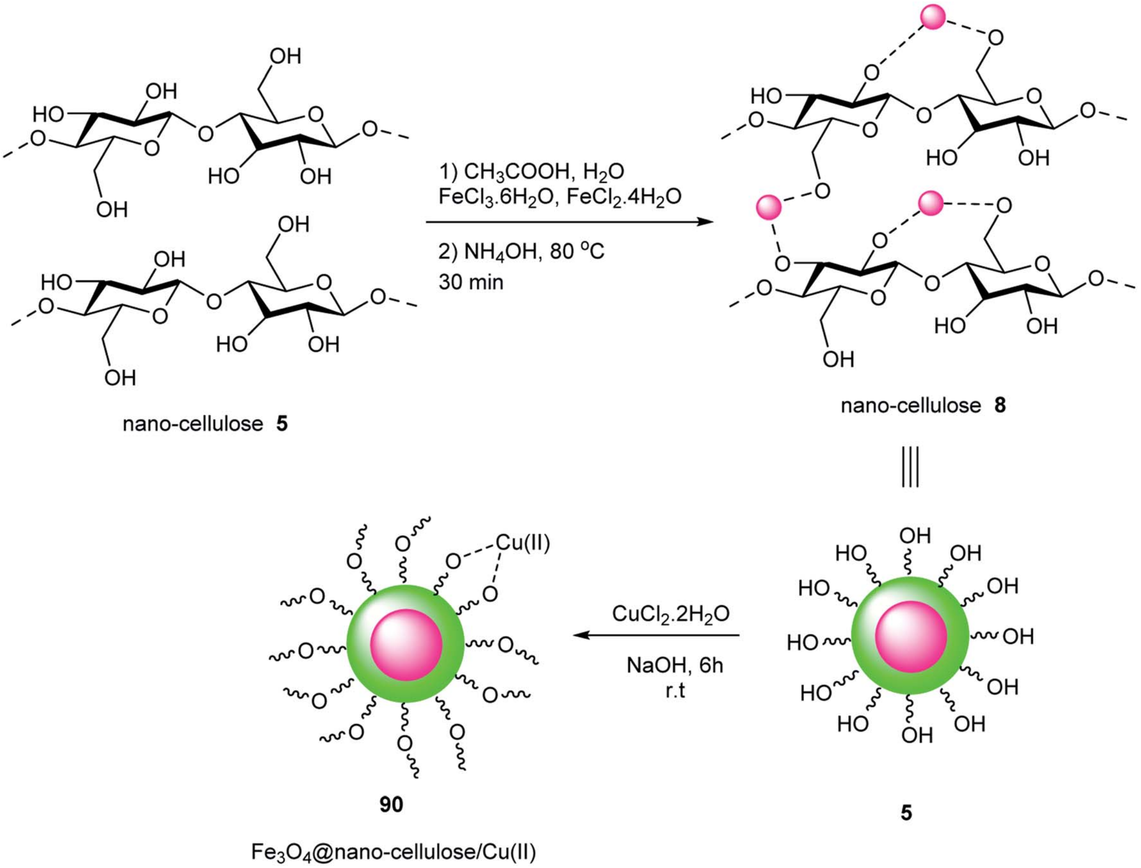

Scheme 24 Synthesis of Fe_3O_4@nano-cellulose/Cu(II).

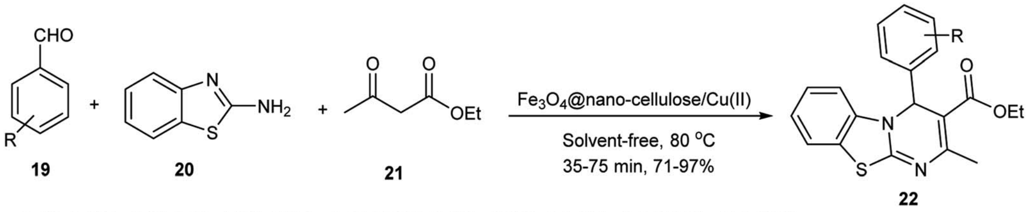

R= H, 4-NO$_2$, 4-Cl, 4-Br, 4-OH, 2-NO$_2$, 2-Cl, 2-OEt, 3-NO$_2$, 3-OH, 2,4-(Cl)$_2$, 2,4-(OMe)$_2$, 3,4-(OH)$_2$

Scheme 25 Synthesis of 4*H*-pyrimido[2,1-*b*]benzothiazole derivatives **22** using Fe_3O_4@nano-cellulose/Cu(II).

Open Access Article. Published on 26 April 2022. Downloaded on 7/17/2025 7:12:56 PM.
This article is licensed under a Creative Commons Attribution-NonCommercial 3.0 Unported Licence.

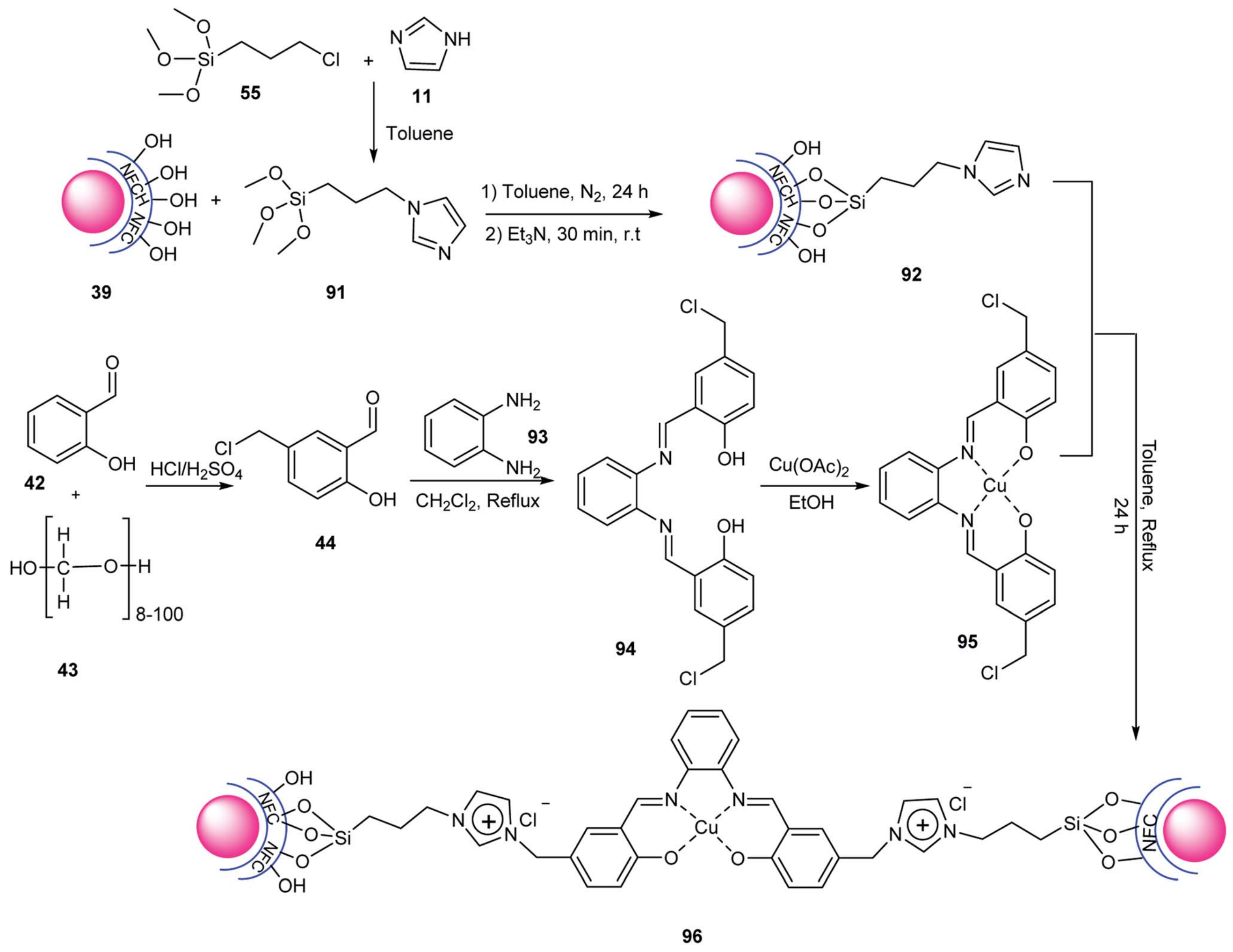

Scheme 26 Synthesis of 4H-pyrimido[2,1-*b*]benzothiazole derivatives using Fe_3O_4@NFC-ImSalophCu(II) **96**.

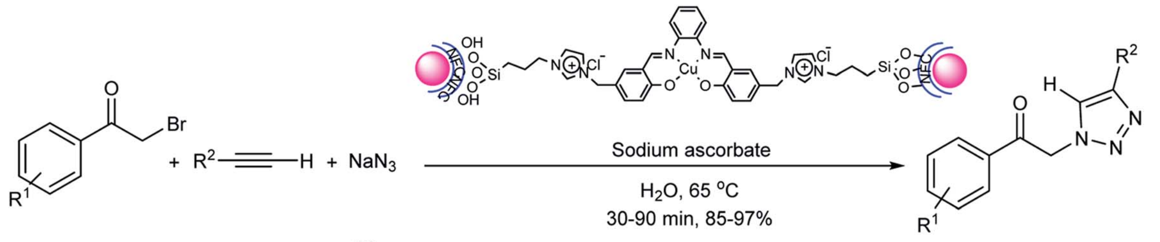

Scheme 27 Synthesis of 1,2,3-triazoles **99** using Fe_3O_4@NFC-ImSalophCu.

aldehydes **19**, dimedone **64**, and 2-aminobenzimidazole **153** or phthalhydrazide **154** to synthesize tetrahydrobenzimidazo[2,1-*b*]quinazolin-1(2*H*)-ones **155** or 2*H*-indazolo[2,1-*b*]phthalazine-trione **156** (Scheme 46). This catalyst was used seven times without loss in any of its activities.[71]

2.4. Magnetic bio-polymers based on alginate

2.4.1. Synthesis and application of Fe_3O_4@-Alg@CPTMS@Arg. Alginate **157** was immobilized on Fe_3O_4 **4** *via* the co-precipitation method. Initially, $FeCl_3\cdot6H_2O$ **1**, $FeCl_2\cdot4H_2O$ **2**, and sodium alginate **157** were dissolved in H_2O under a nitrogen atmosphere. Then, an ammonia solution was added to this mixture to give Fe_3O_4@Alg nanoparticles **158**, which were functionalized with 3-chloropropyltrimethoxysilane **55** to prepare Fe_3O_4@Alg@CPTMS **159**, followed by reaction with *L*-arginin **160** using trimethylamine in EtOH for 48 h to give Fe_3O_4@Alg@CPTMS@Arg **161** (Scheme 47).[72]

Open Access Article. Published on 26 April 2022. Downloaded on 7/17/2025 7:12:56 PM.
This article is licensed under a Creative Commons Attribution-NonCommercial 3.0 Unported Licence.

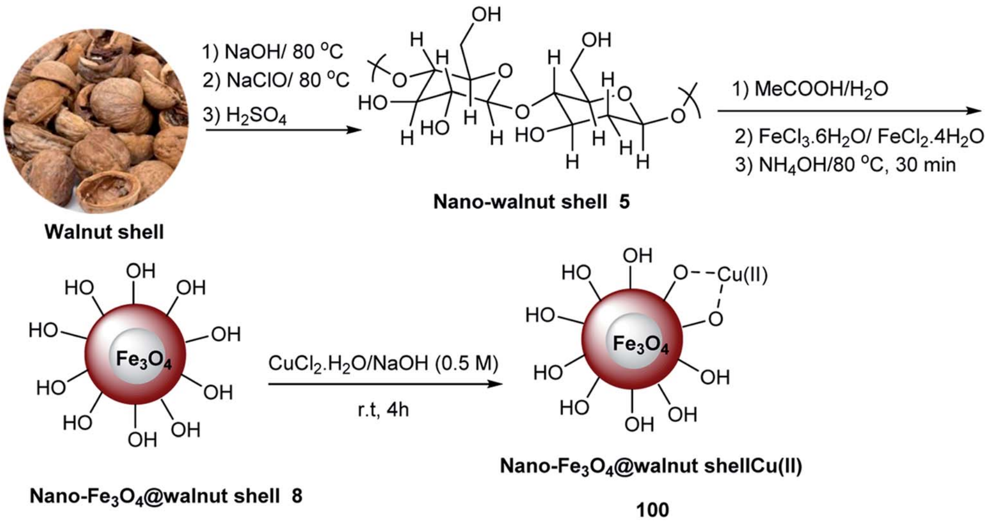

Scheme 28 Synthesis of nano-Fe_3O_4@walnut shell/Cu.

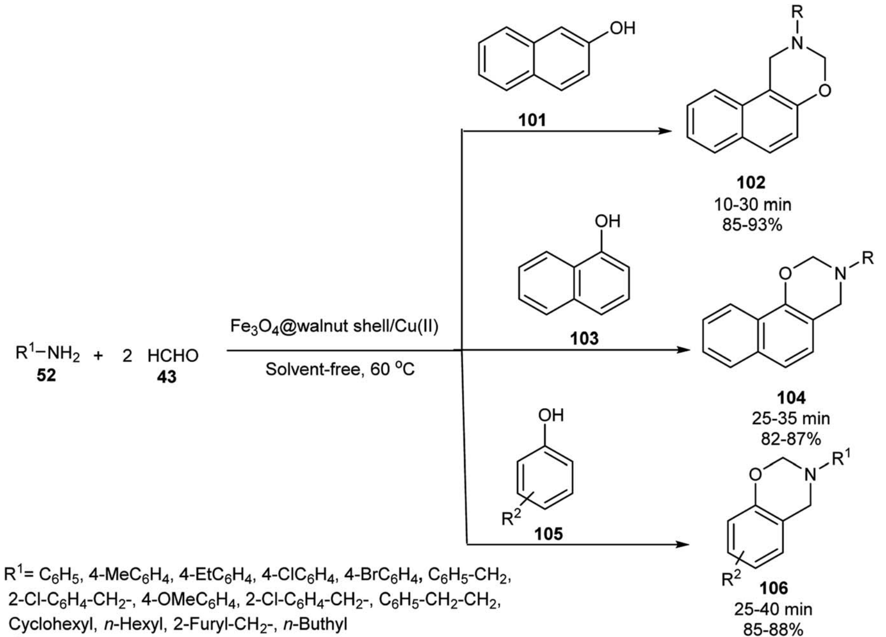

Scheme 29 Synthesis of 2-aryl/alkyl-2,3-dihydro-1*H*-naphtho[1,2-*e*][1,3]oxazines **102** or **104** or **106** using nano-Fe_3O_4@walnut shell/Cu(II).

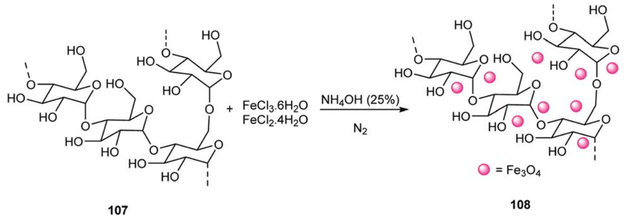

Scheme 30 Synthesis of magnetic dextrin.

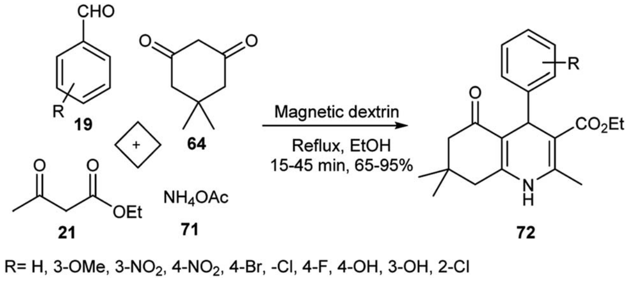

Scheme 31 Synthesis of polyhydroquinolines **72** in the presence of magnetic dextrin.

Open Access Article. Published on 26 April 2022. Downloaded on 7/17/2025 7:12:56 PM. This article is licensed under a Creative Commons Attribution-NonCommercial 3.0 Unported Licence.

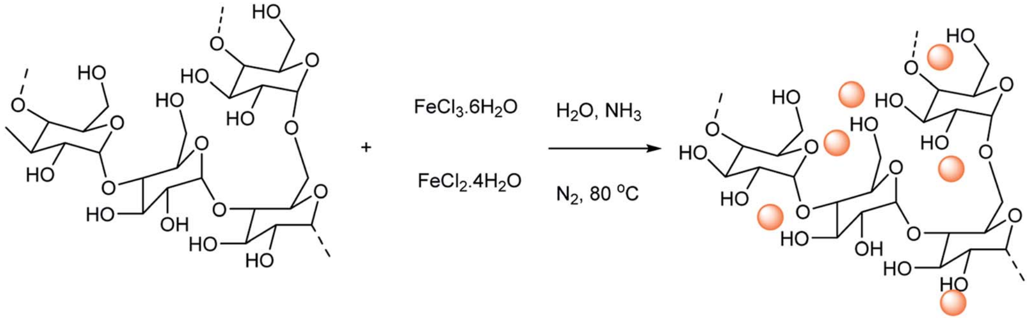

Scheme 32 Synthesis of magnetized dextrin.

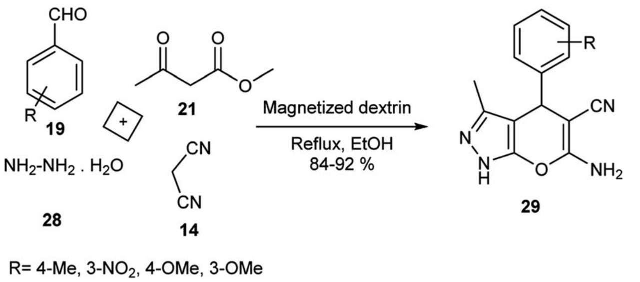

Scheme 33 Synthesis of dihydropyrano[2,3-*c*]pyrazoles **29** using magnetized dextrin.

Subsequently, Fe_3O_4@Alg@CPTMS@Arg, which has two acidic and basic functional sites, activated the carbonyl groups in the synthesis of 2,4,5-triarylimidazoles through the reaction of ammonium acetate, aldehydes, and benzil in EtOH under reflux conditions (Scheme 48). The recyclability of the catalyst was tested 7 times using the model reaction without loss in any of its activities. When Fe_3O_4 was used as the catalyst, the yield of this reaction was about 65%.[72]

2.4.2. Synthesis and application of Fe_3O_4@Alg@CPTMS@Arg. The reaction of Fe_3O_4@Alg **165** and 3-chloropropyltrimethoxysilane (CPTMS) **55** in toluene under reflux conditions and nitrogen atmosphere gave Fe_3O_4@Alg@CPTMS **166**, which was reacted with arginine **167** in the presence of trimethylamine in dry toluene to provide Fe_3O_4@Alg@CPTMS@Arg nanocomposites **168** (Scheme 49).[73]

The activity of Fe_3O_4@Alg@CPTMS@Arg was tested as a catalyst in the synthesis of 2,4,5-triarylimidazoles **36** *via* the reaction of ammonium acetate **71,** aldehyde derivatives **19,** and benzil **34** in EtOH (Scheme 50). Its catalytic activity did not decrease after seven uses. It has two functional groups including a Lewis base (NH_2) and Brønsted acidic (COOH), which catalyzed the synthesis of 2,4,5-triarylimidazoles.[73]

2.4.3. Synthesis and application of Fe_3O_4@FU. Fe_3O_4@FU **170** was prepared *via* the reaction of fucoidan powder **169,**

Scheme 34 Synthesis of FND-Ti(IV) **109**.

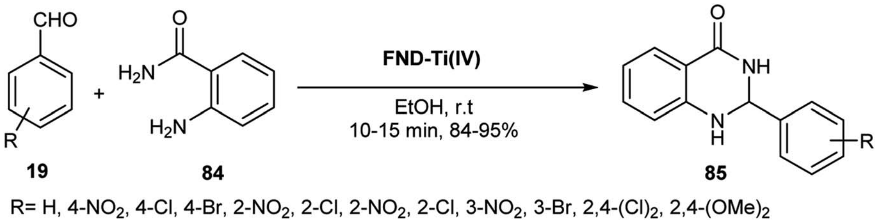

Scheme 35 Synthesis of 2,3-dihydroquinazolin-4(1*H*)-ones **85** using Fe_3O_4@nano-dextrin/Ti(IV).

Open Access Article. Published on 26 April 2022. Downloaded on 7/17/2025 7:12:56 PM.
This article is licensed under a Creative Commons Attribution-NonCommercial 3.0 Unported Licence.

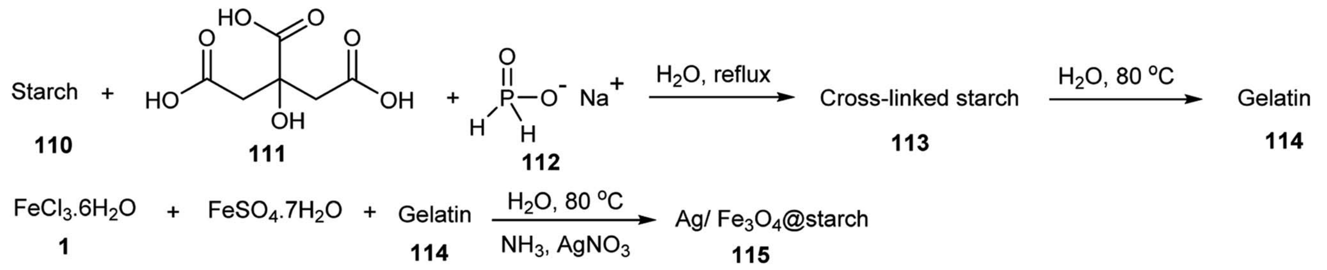

Scheme 36 Synthesis of Ag/Fe_3O_4@starch **115**.

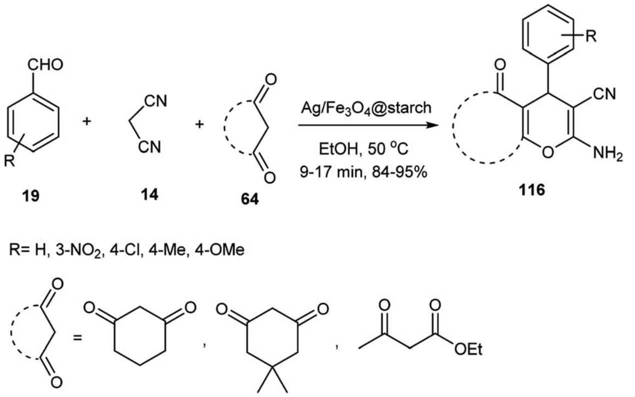

Scheme 37 Synthesis of 4*H*-pyran **116** in the presence of Ag/Fe_3O_4@starch.

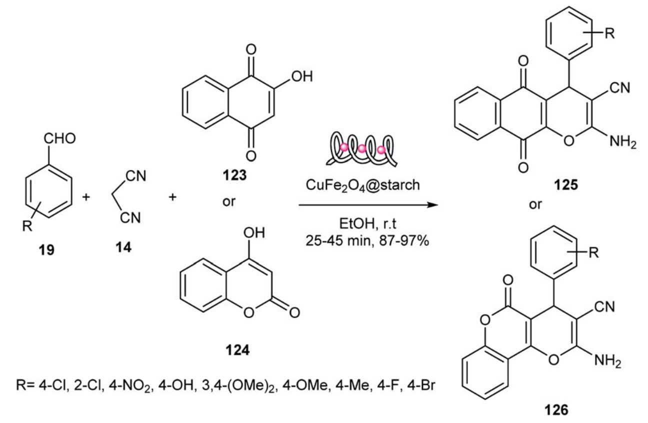

Scheme 39 Synthesis of 4*H*-chromenes using $CuFe_2O_4$@starch.

$FeCl_2\cdot4H_2O$ **2**, and $FeCl_3\cdot6H_2O$ **1** in aqueous ammonia solution (25%) in distilled water under a nitrogen atmosphere at 80 °C (Scheme 51).[74]

The activity of Fe_3O_4@FU was evaluated as a catalyst in the synthesis of *tri*- and *tetra*-substituted imidazoles **36** or **171** *via* three- and four-component reactions of benzil **34**, aldehydes **19**, NH_4OAc **71**, and amine **52** under reflux conditions in EtOH (Scheme 52), respectively. The catalyst was used six times in the model reaction without loss in any of its activities. This reaction was accomplished in ethanol under reflux conditions in the presence of Fe_3O_4 as a catalyst after 40 min with 55% yield. The carbonyl groups were activated *via* hydrogen bonding with Fe_3O_4@FU as a catalyst.[74]

2.5. Magnetic bio-polymers based on glucose

2.5.1. Synthesis and application of Fe_3O_4@C@ONa.

Initially, $FeCl_3$–$6H_2O$ solution, $CO(NH_2)_2$, and glucose were added to ethylene glycol **172** to produce a black powder of carbon-coated magnetic nanoparticles (CCMNPs: Fe_3O_4@C) **173**, followed by reaction with NaOH solution to obtain basic carbon-coated magnetic nanoparticles (BCCMNPs: Fe_3O_4@C@ONa) **174** (Scheme 53).[75]

Subsequently, the catalytic activity of Fe_3O_4@C@ONa was tested for the synthesis of 4*H*-chromene derivatives **174** *via* the reaction of salicylaldehyde **42**, dimedone **64**, and β-naphthol **101** in water at 60 °C (Scheme 54). Also, the catalyst was used five times in the model reaction without loss in any of its

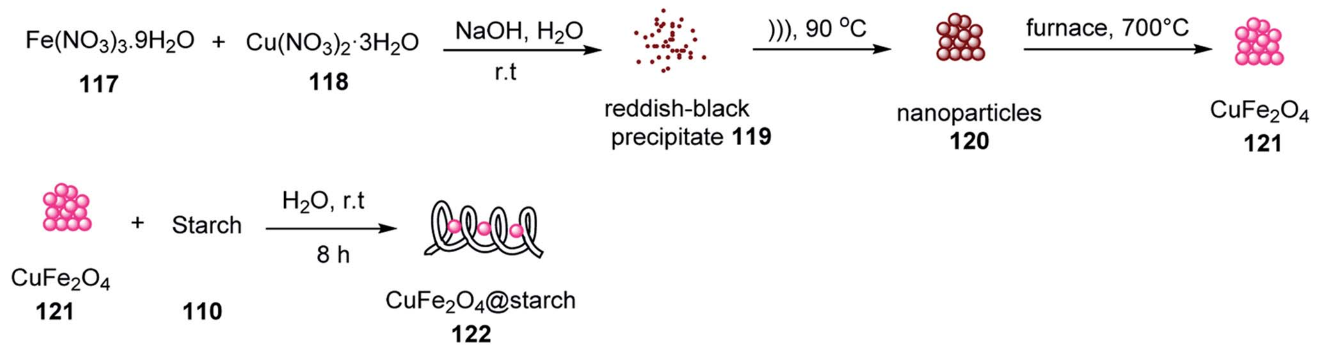

Scheme 38 Synthesis of $CuFe_2O_4$@starch.

Open Access Article. Published on 26 April 2022. Downloaded on 7/17/2025 7:12:56 PM. This article is licensed under a Creative Commons Attribution-NonCommercial 3.0 Unported Licence.

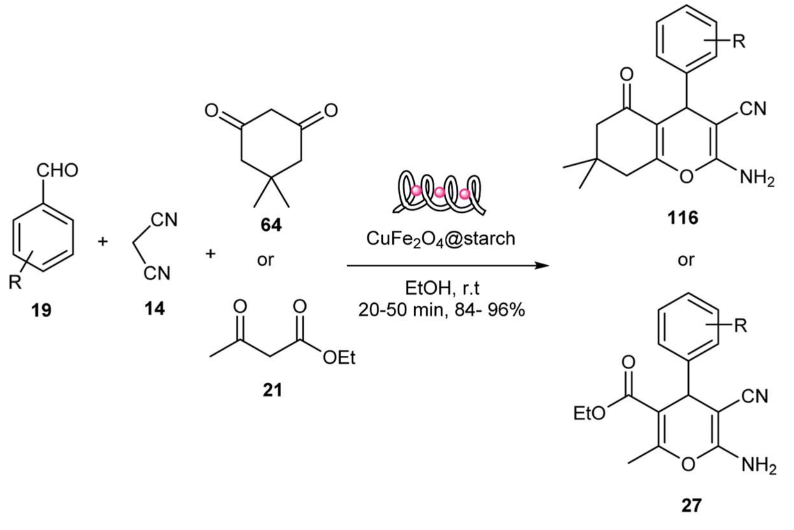

R= 4-Cl, 4-NO$_2$, 2-NO$_2$, 3-Br, 4-OH, 4-N(Me)$_2$, 2-OH-3-OMe, 3-NO$_2$, 3-OMe, 2,4-(Cl)$_2$, 4-Me, 3-Cl, 2-Cl

Scheme 40 Synthesis of 2-amino-5-oxo-5,6,7,8-tetrahydro-4*H*-benzo[*b*]pyrans **116** or **27**.

activities. This catalyst has two functional groups, including Fe^{3+} as a Lewis acid and oxygen group as a Lewis base, which increased the reaction rate.[75]

2.6. Magnetic bio-polymers based on chitosan

2.6.1. Synthesis and application of CSSNH@Arg.

Chitosan-silica sulfate nanohybrid (CSSNH@Arg) **178** was synthesized *via* the reaction of chitosan **176** and silica sulfuric acid (SSA) **177** under ultrasonic irradiation (Scheme 55).[76]

A green method for the synthesis of 3,4-dihydropyrimidine-2(1*H*)-one/thione derivatives **179** was described by Behrouz and co-workers *via* the Biginelli reaction of (thio)urea **23** or urea **6**, methyl acetoacetate **21**, and aldehydes **19** using CSSNH@Arg **178** under solvent-free conditions (Scheme 56).

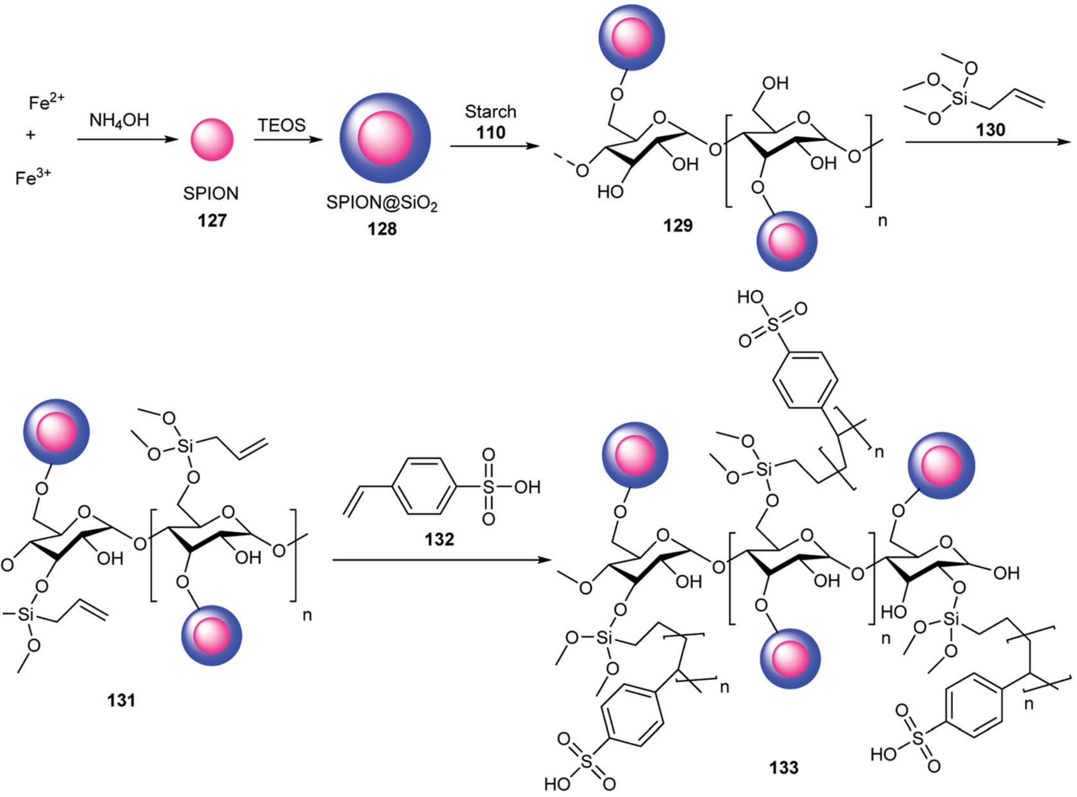

Scheme 41 Synthesis of starch/SPION@SO$_3$H.

Open Access Article. Published on 26 April 2022. Downloaded on 7/17/2025 7:12:56 PM.
This article is licensed under a Creative Commons Attribution-NonCommercial 3.0 Unported Licence.

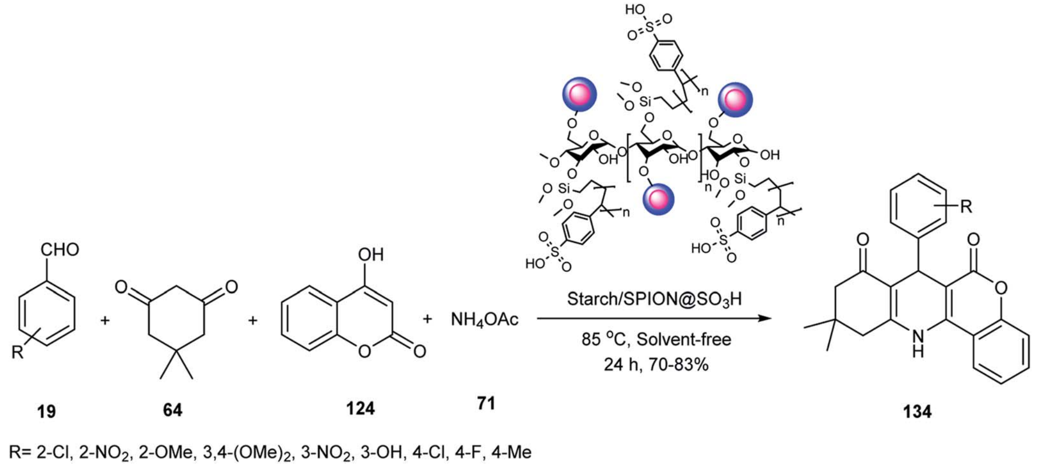

Scheme 42 Synthesis of chromeno[4,3-*b*]quinoline-6,8(9*H*)-diones in the presence of Starch/SPION@SO_3H.

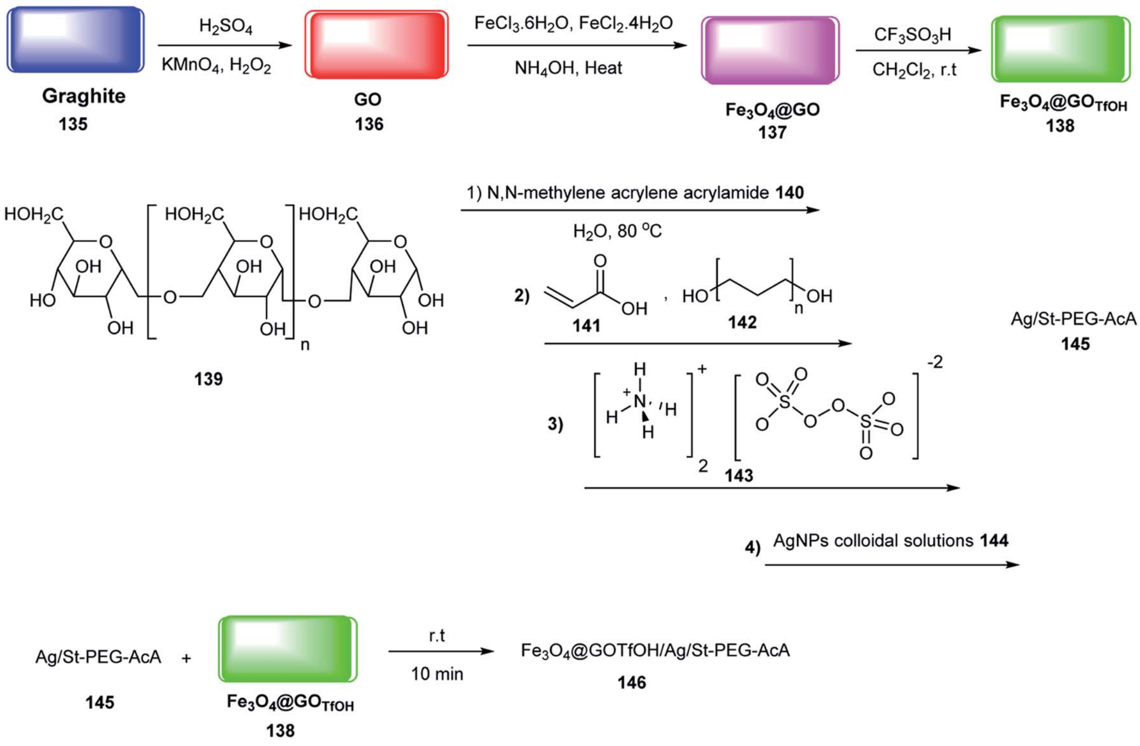

Scheme 43 Synthesis of Fe_3O_4@GOTfOH/Ag/St-PEG-AcA **146**.

According to the reusability test, this catalyst was used five times without a decrease in any of its activities. The various functional groups including hydroxyl and amine on the CSSNH@Arg can activate the carbonyl groups *via* hydrogen bonding.[76]

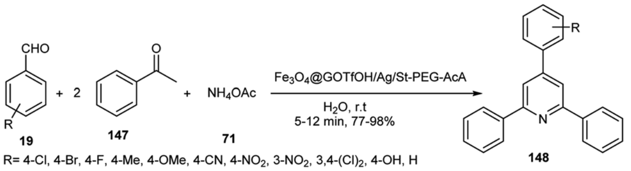

Scheme 44 Synthesis of 2,4,6-triarylpyridine derivatives **148** using Fe_3O_4@GOTfOH/Ag/St-PEG-AcA.

2.6.2. Synthesis and application of Fe_3O_4@C–SO_3H. Initially, starch was mixed with sulfuric acid, and then the reaction mixture was transferred to an autoclave for 24 h at 180 °C, resulting in the formation of a solid black product (C–SO_3H). The magnetic Fe_3O_4 nanoparticles, carbon-based solid acid (C–SO_3H) **180**, and H_2O were placed in an oil bath at 100 °C to remove H_2O, and then the reaction mixture was poured into a Teflon-sealed autoclave and heated at 180 °C for 6 h to achieve Fe_3O_4@C–SO_3H **181** (Scheme 57).[77]

Open Access Article. Published on 26 April 2022. Downloaded on 7/17/2025 7:12:56 PM. This article is licensed under a Creative Commons Attribution-NonCommercial 3.0 Unported Licence.

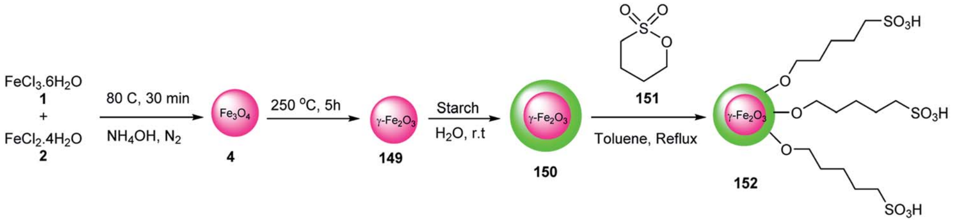

Scheme 45 Synthesis of γ-Fe_2O_3@starch-*n*-butyl SO_3H.

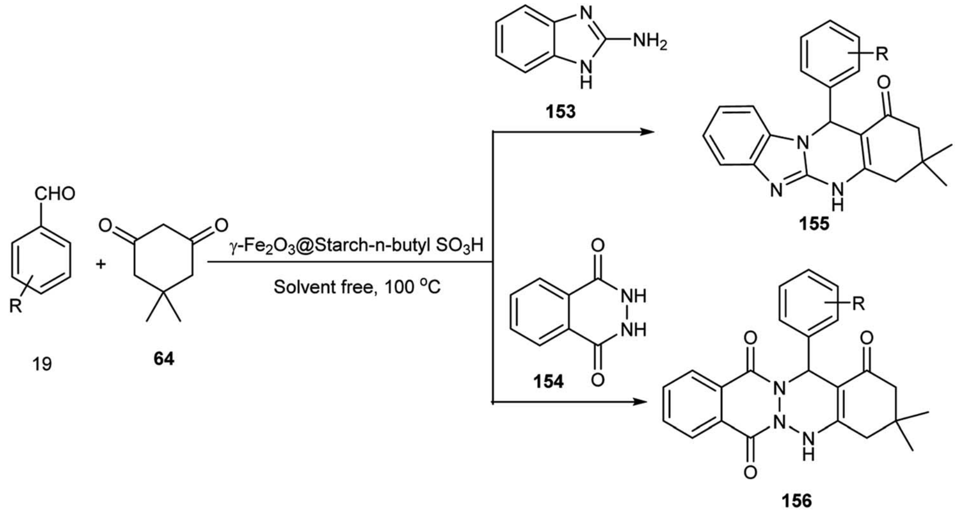

Scheme 46 Synthesis of tetrahydrobenzimidazo[2,1-*b*]quinazolin-1(2*H*)-ones **155** or 2*H*-indazolo[2,1-*b*]phthalazine-triones **156** using γ-Fe_2O_3@starch-*n*-butyl SO_3H.

CSSNH was applied as a Brønsted acid catalyst in the synthesis of 2-amino-3-cyano-4*H*-pyrans **126** and 2-amino-4*H*-chromenes **116** or **182** *via* the three-component reactions of malononitrile **14**, benzaldehyde **19**, and β-naphthol **101** or dimedone **64** or 4-hydroxycoumarin **124**, respectively (Scheme 58). This catalyst was used four times without any loss in its activity.[77]

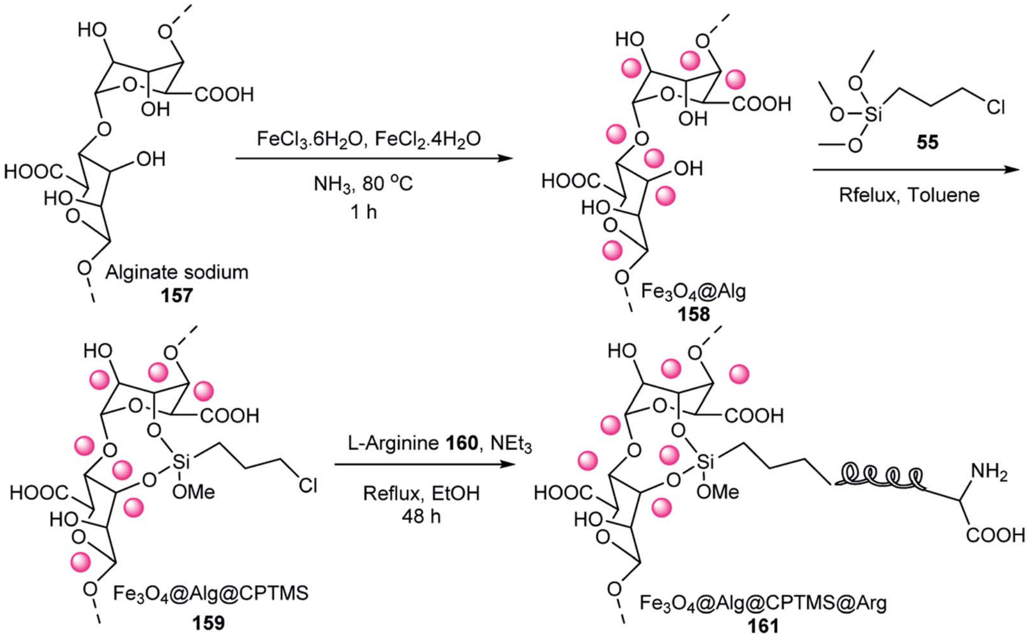

Scheme 47 Synthesis of Fe_3O_4@Alg@CPTMS@Arg **161**.

© 2022 The Author(s). Published by the Royal Society of Chemistry

Open Access Article. Published on 26 April 2022. Downloaded on 7/17/2025 7:12:56 PM. This article is licensed under a Creative Commons Attribution-NonCommercial 3.0 Unported Licence.

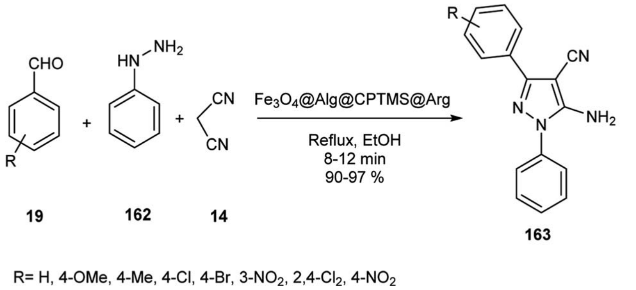

Scheme 48 Synthesis of 2,4,5-triarylimidazoles **163** using Fe_3O_4@Alg@CPTMS@Arg.

2.6.3. Synthesis and application of magnetic chitosan-terephthaloyl-creatine bio-nanocomposite. The reaction of terephthaloyl chloride **183** and creatine powders **184** in CH_2Cl_2 under reflux conditions provided creatine-terephthaloyl chloride ligand **185**, which was added to chitosan **176** powder in a hydrochloric acid solution, and then refluxed to give chitosan-terephthaloyl-creatine bio-nanocomposite **186**, followed by immobilization on Fe_3O_4 to provide magnetic chitosan-terephthaloyl-creatine bio-nanocomposite **187** (Scheme 59).[78]

Its catalytic activity was tested in the synthesis of polyhydroquinolines **72** *via* the reaction of aldehydes **19**, dimedone **67**, ammonium acetate **71**, and ethyl acetoacetate or methyl acetoacetate **21** in EtOH (Scheme 60). In another attempt, it was used in the synthesis of 1,4-dihydropyridines **73** *via* the pseudo-three-component reaction of aldehydes **19**, methyl acetoacetate **21**, and ammonium acetate **71** (Scheme 61). The acidic site of the catalyst activated the carbonyl groups of the primary compounds. The activity of this catalyst did not decrease after use eight times.[78]

2.6.4. Synthesis and application of magnetic cyanoguanidine-modified chitosan (MCGC). Firstly, chitosan **176** was obtained *via* the deacetylation of chitin **74**, and then it was modified by treatment with cyanoguanidine **188** in HCl solution to produce cyanoguanidine-modified chitosan (CGC) **189**, which was immobilized on Fe_3O_4 nanoparticles to afford magnetic cyanoguanidine-modified chitosan (MCGC) **190** (Scheme 62). Its catalytic activity was investigated in the synthesis of benzimidazoloquinazolines **155** *via* the reaction of aldehydes **19**, 2-aminobenzimidazole **153**, and dimedone **64** in EtOH under reflux conditions. The sonochemical method afforded better yields in shorter reaction times than the conventional method (Scheme 63).[79]

1,4-Dihydropyridines **73** were synthesized *via* the Hantzsch reaction of ethyl acetoacetate **35**, aromatic aldehydes **19**, and ammonium acetate **71** under ultrasonic irradiation in the presence of MCGC **190** as a catalyst, which activated the carbonyl groups *via* hydrogen bonding. Also, the yield of the reaction did not decrease after eight times usage of the catalyst (Scheme 64).[79]

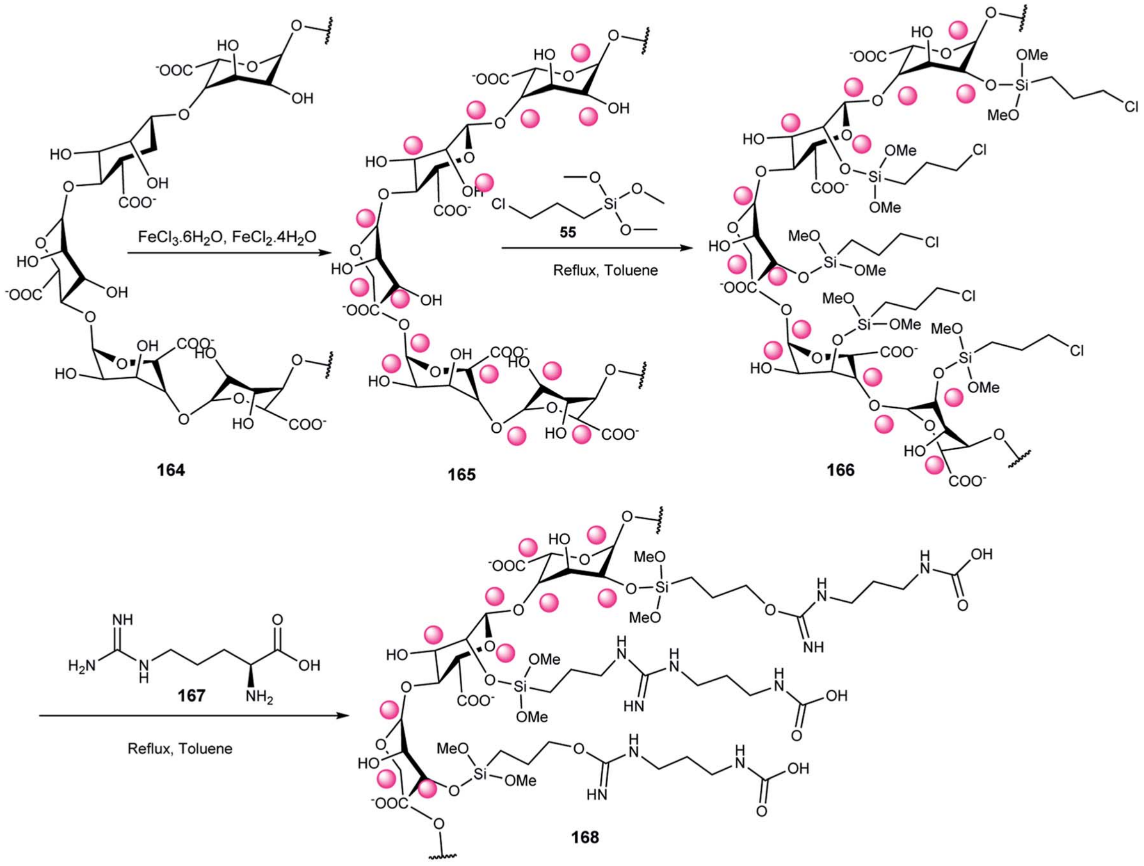

Scheme 49 Synthesis of Fe_3O_4@Alg@CPTMS@Arg.

Open Access Article. Published on 26 April 2022. Downloaded on 7/17/2025 7:12:56 PM.
This article is licensed under a Creative Commons Attribution-NonCommercial 3.0 Unported Licence.

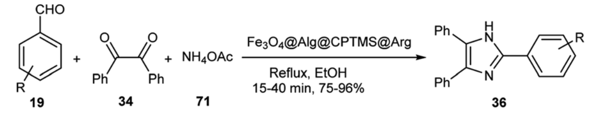

R= 4-Cl, 2-OH, 3,4-(OH)2, 2-Cl, 2-Cl, 4-Me, 2-COOH, 4-N(Me)$_2$, 4-N(Me)$_2$, 4-OH, 4-CN, 4-NO$_2$, 2,4-(Cl)$_2$

Scheme 50 Synthesis of 2,4,5-triarylimidazoles derivatives in the presence of Fe_3O_4@Alg@CPTMS.

2.6.5. Synthesis and application of magnetic $MnFe_2O_4$-CS-Bu-SO_3H. Manganese ferrite nanoparticles were synthesized *via* the co-precipitation of Fe(III) **1** and Mn(II) **189** in the presence of NaOH solution at 97 °C to give $MnFe_2O_4$ **191**, which was immobilized on chitosan **176** and 4-butane sultone **151** to prepare $MnFe_2O_4$-CS-Bu-SO_3H **192** (Scheme 65).[80]

The catalyst activity of $MnFe_2O_4$-CS-Bu-SO_3H was investigated in the synthesis of *spiro*[acenaphthylene-1,9′-acridine]

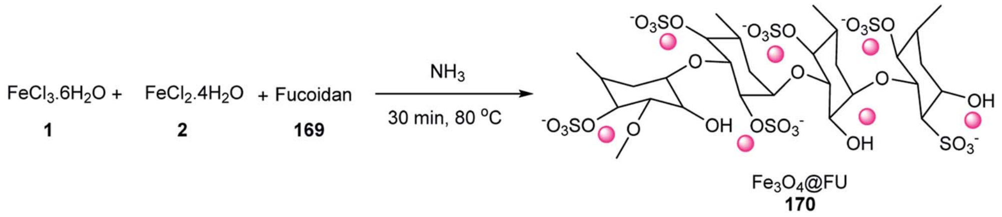

Scheme 51 Synthesis of magnetic Fe_3O_4@FU **170**.

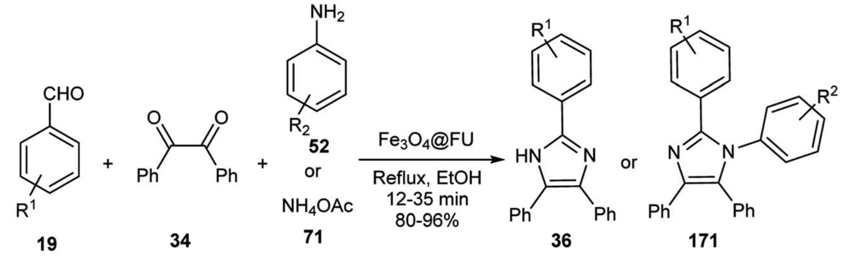

R^1= H, 4-Cl, 2-Cl, 4-CN, 2,4-(Cl)$_2$, 2-COOH, 4-OH, 4-NO$_2$, 3-NO$_2$, 4-NMe$_2$, 4-Me, 4-OMe, 4-NO$_2$, 3-NO$_2$, 4-OH
R^2= H, 4-Me

Scheme 52 Synthesis of imidazole derivatives.

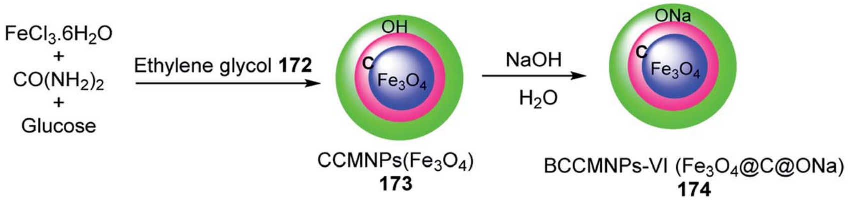

Scheme 53 Synthesis of Fe_3O_4@C@ONa.

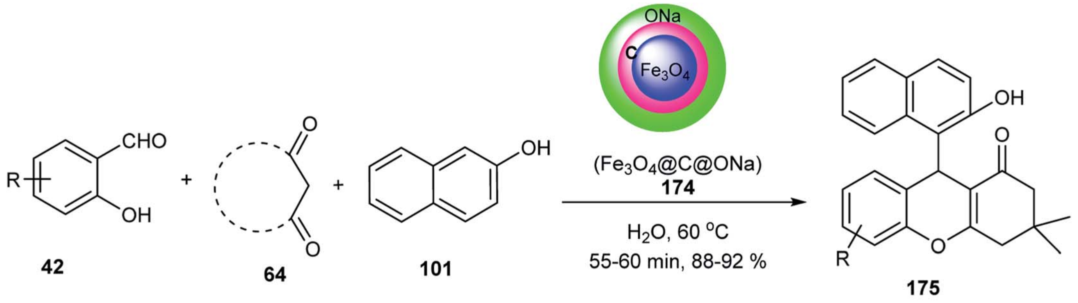

R= H, 3-OMe, 4-OMe, 5-NO$_2$, 4-Br, 4-OMe

Scheme 54 Synthesis of 4*H*-chromene derivatives using Fe_3O_4@C@ONa **174**.

Open Access Article. Published on 26 April 2022. Downloaded on 7/17/2025 7:12:56 PM.
This article is licensed under a Creative Commons Attribution-NonCommercial 3.0 Unported Licence.

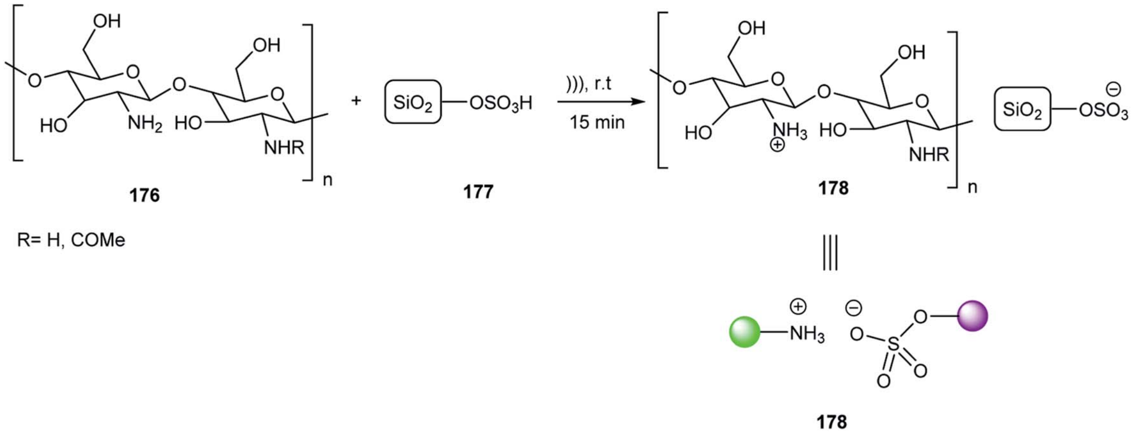

Scheme 55 Synthesis of CSSNH@Arg **178**.

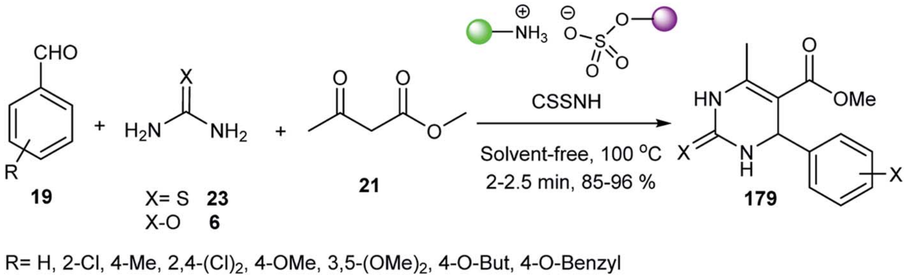

Scheme 56 Synthesis of 3,4-dihydropyrimidine-2(1*H*)-(thio)ones using of CSSNH@Arg **178**.

triones **194** *via* the multicomponent reaction of dimedone **64**, aldehydes **19**, and acenaphthoquinone **193** under ultrasonic irradiation in H_2O (Scheme 66). Also, $MnFe_2O_4$-CS-Bu-SO_3H as a Brønsted acid increased the reaction rate *via* hydrogen bonding with the carbonyl group. According to the reusability test, this catalyst was used five times without any loss in its activity.[80]

2.6.6. Synthesis and application of magnetic Cu-MCS. Fe_3O_4 NPs **4** were reacted with carboxymethylated chitosan to obtain magnetic chitosan MCS **195**, which was reacted with $CuCl_2 \cdot 2H_2O$ in H_2O to generate Cu NPs@Fe_3O_4-chitosan (Cu-MCS) **196** (Scheme 67).

The catalytic activity of Cu-MCS was verified in the synthesis of various tetrazoles **198** or **199** *via* the reaction of cyanamides **197** and NaN_3 **50** in H_2O under reflux conditions (Scheme 68). This catalyst could be used five times without loss in its activity.[81]

2.6.7. Synthesis and application of magnetic Ch-Fe_3O_4 NCs. Chitosan was dissolved in an acetic acid solution, and then $FeCl_3 \cdot 6H_2O$ **1** and $FeCl_2 \cdot 4H_2O$ **2** were added to the reaction mixture for 6 h at 80 °C under an N_2 atmosphere. Then, NH_4OH

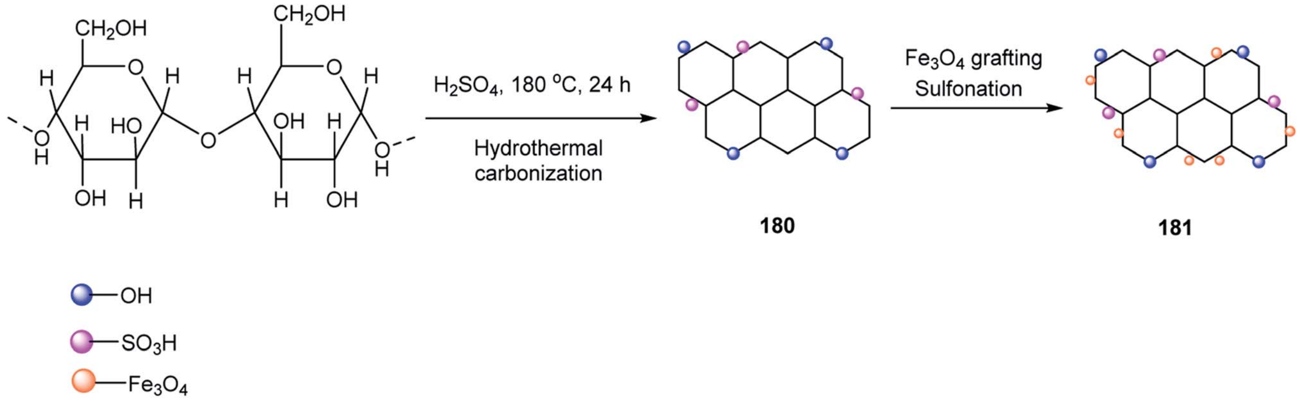

Scheme 57 Synthesis of 3,4-dihydropyrimidine-2(1*H*)-(thio)ones in the presence of CSSNH **178**.

Open Access Article. Published on 26 April 2022. Downloaded on 7/17/2025 7:12:56 PM.
This article is licensed under a Creative Commons Attribution-NonCommercial 3.0 Unported Licence.

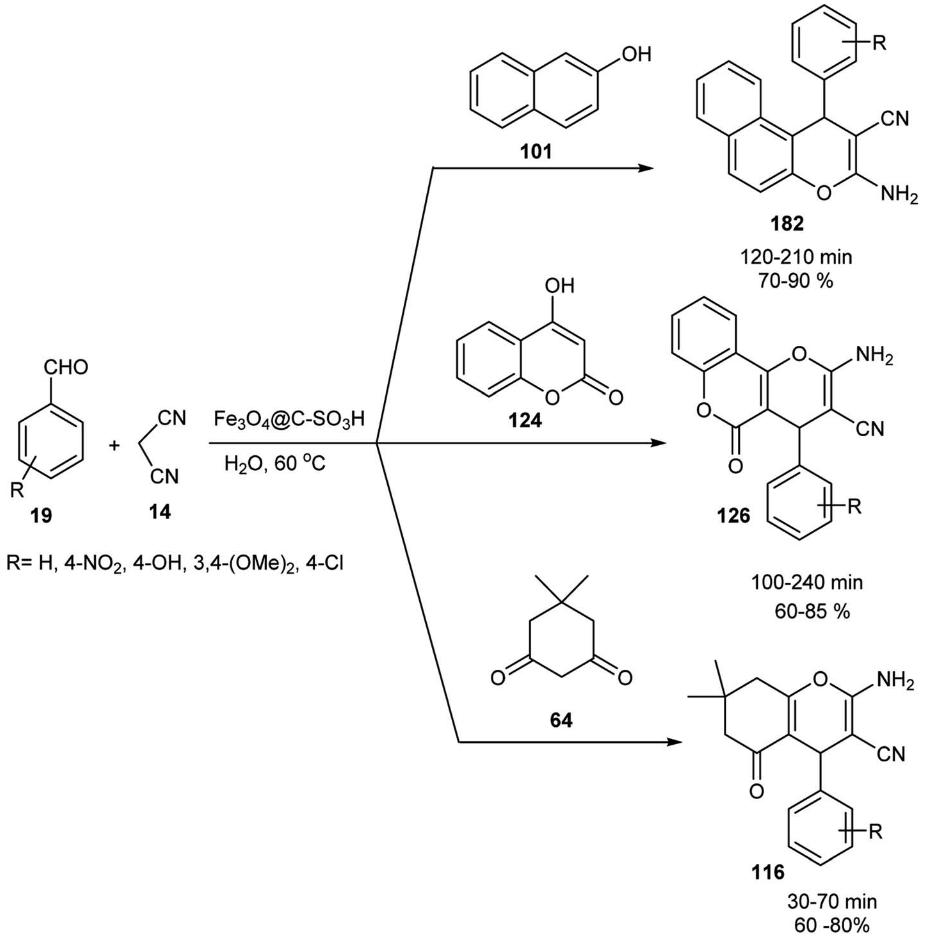

Scheme 58 Synthesis of 2-amino-4*H*-chromenes **116** and 2-amino-3-cyano-4*H*-pyrans **126** in the presence of Fe_3O_4@C–SO_3H.

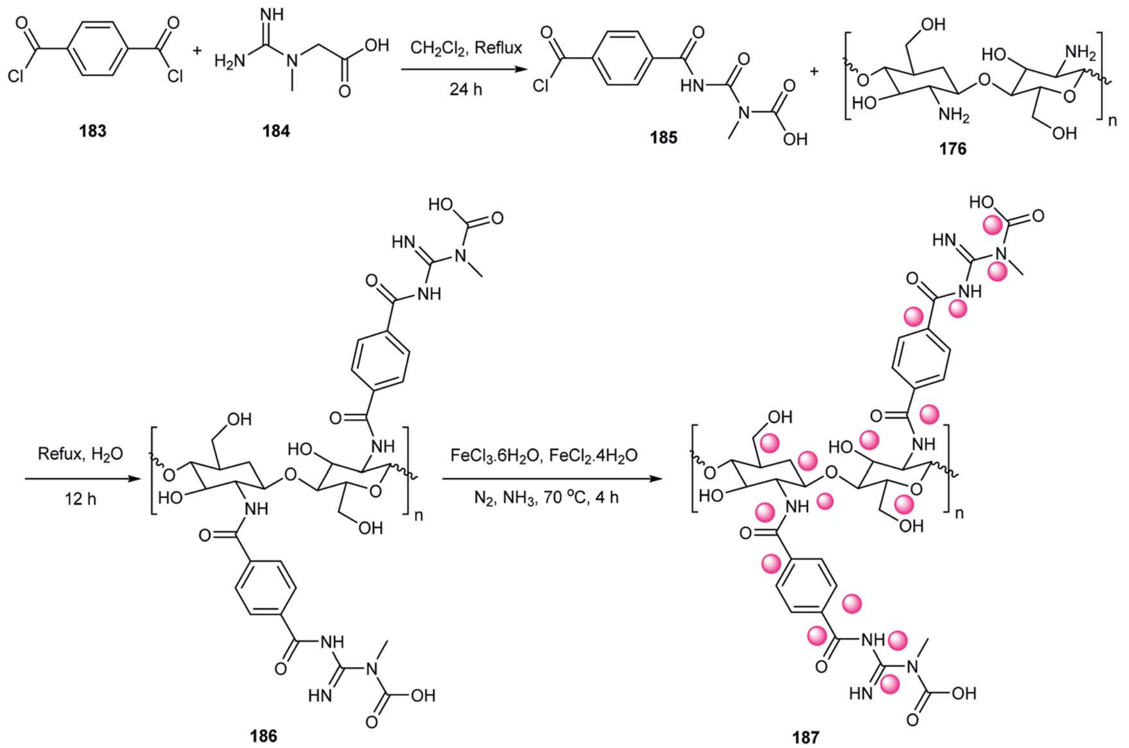

Scheme 59 Synthesis of magnetic chitosan-terephthaloyl-creatine bio-nanocomposite.

Open Access Article. Published on 26 April 2022. Downloaded on 7/17/2025 7:12:56 PM. This article is licensed under a Creative Commons Attribution-NonCommercial 3.0 Unported Licence.

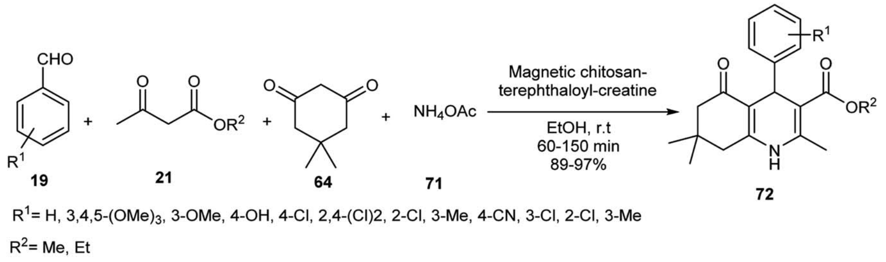

Scheme 60 Synthesis of polyhydroquinoline derivatives **72**.

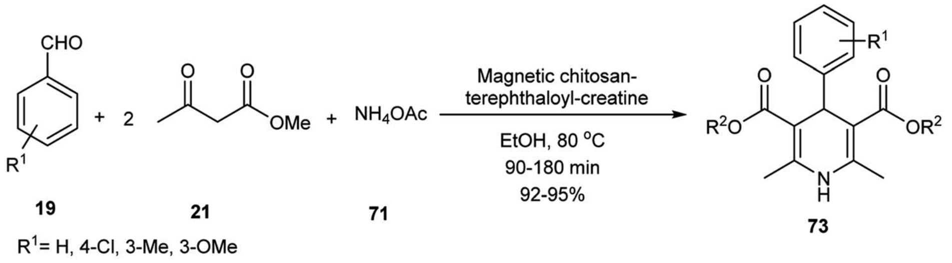

Scheme 61 Synthesis of 1,4-dihydropyridine derivatives **73** in the presence of terephthaloyl-creatine bio-nanocomposite.

was added to the reaction mixture to obtain Ch-Fe$_3$O$_4$ NCs **200**. Finally, the chitosan magnetic nanocomposite of Ch-rhomboclase NCs **201** was synthesized *via* the reaction of Ch-Fe$_3$O$_4$ NCs **200** with chlorosulfonic acid at room temperature under N$_2$ gas (Scheme 69).[82]

The condensation reaction of benzaldehyde **19**, ethyl acetoacetate **35** or dimedone **64**, and ammonium acetate **71** gave 1,4-dihydropyridine derivatives **73** or **202** in the presence of Ch-rhomboclase NCs **201** under solvent-free conditions at 80 °C (Scheme 70). In the Hantzsch reaction, this acidic catalyst activated carbonyl groups *via* hydrogen bonding. Also, according to the reusability test, the catalyst was used seven times without any decrease in its activity.[82]

2.6.8. Synthesis and application of magnetic Fe$_3$O$_4$/CS/COF/Cu. After the preparation of an FeCl$_3$·6H$_2$O solution in ethylene glycol at room temperature, chitosan, sodium acetate,

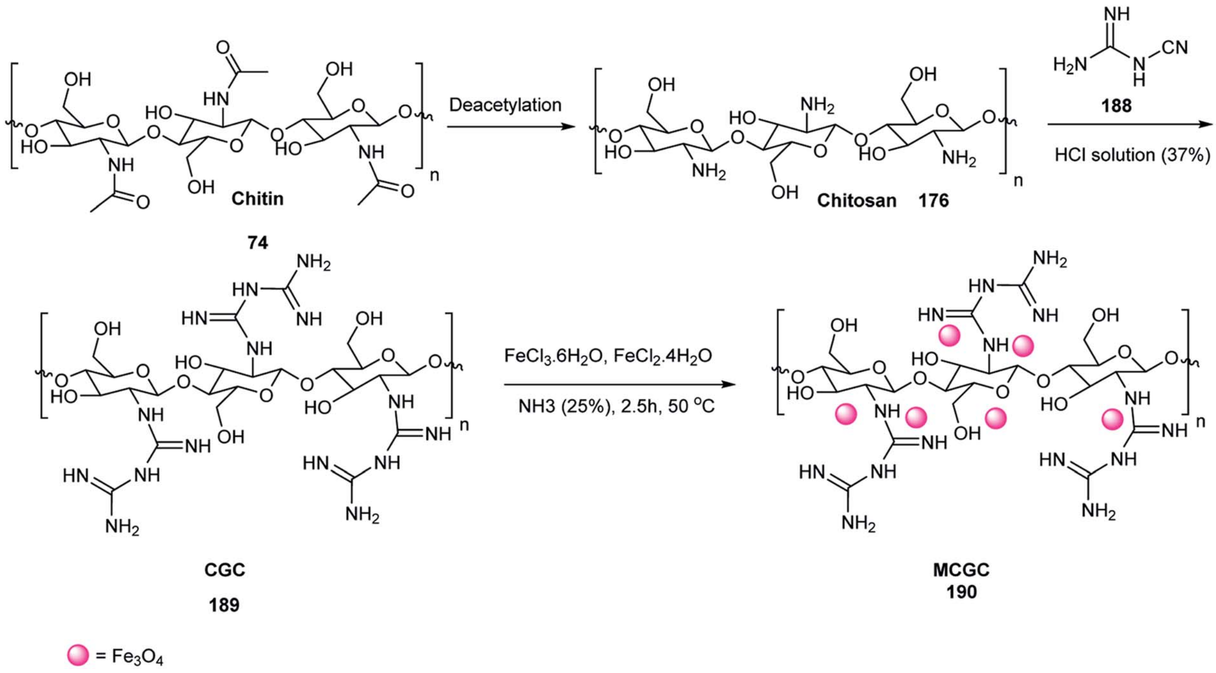

Scheme 62 Synthesis of magnetic cyanoguanidine-modified chitosan (MCGC).

Open Access Article. Published on 26 April 2022. Downloaded on 7/17/2025 7:12:56 PM.
This article is licensed under a Creative Commons Attribution-NonCommercial 3.0 Unported Licence.

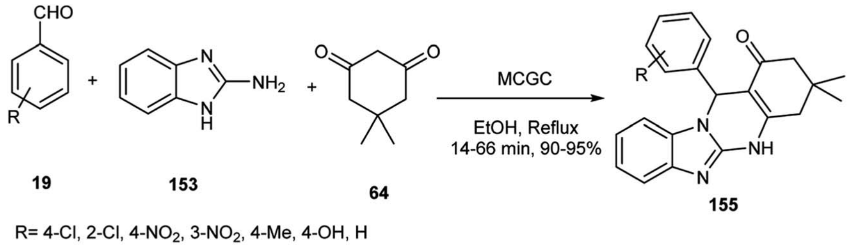

Scheme 63 Synthesis of benzimidazoloquinazoline derivatives.

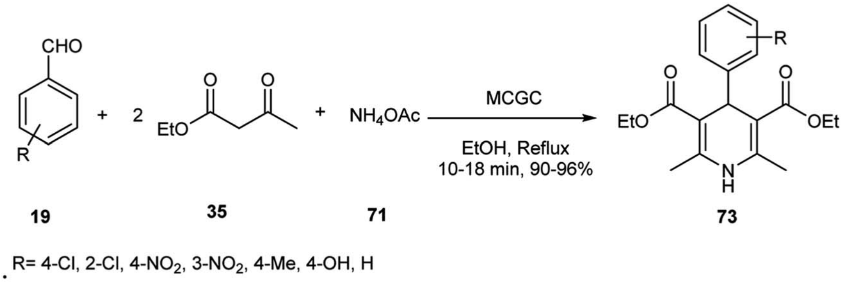

Scheme 64 Synthesis of 1,4-dihydropyridines.

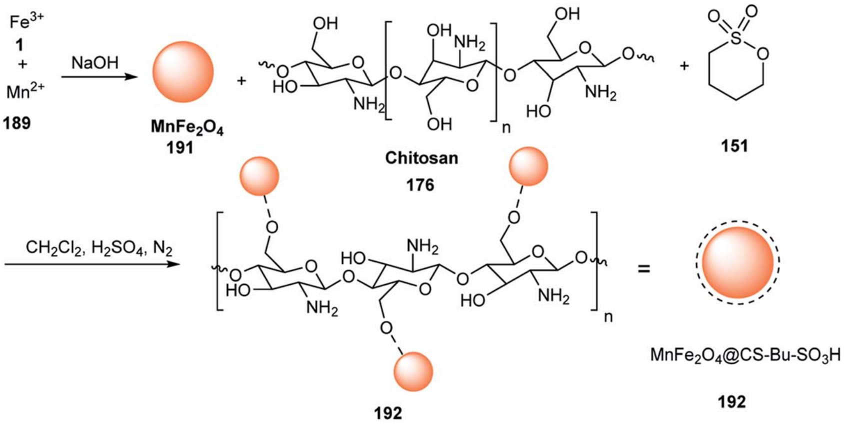

Scheme 65 Synthesis of $MnFe_2O_4$-CS-Bu-SO_3H **192**.

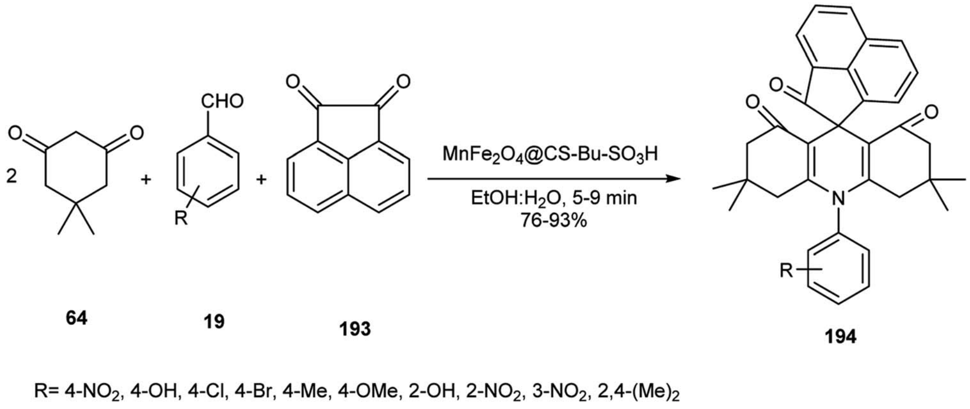

Scheme 66 Synthesis of spiro[acenaphthylene-1,9′-acridine] triones **194** in the presence of $MnFe_2O_4$@CS-Bu-SO_3H NPs.

Open Access Article. Published on 26 April 2022. Downloaded on 7/17/2025 7:12:56 PM.
This article is licensed under a Creative Commons Attribution-NonCommercial 3.0 Unported Licence.

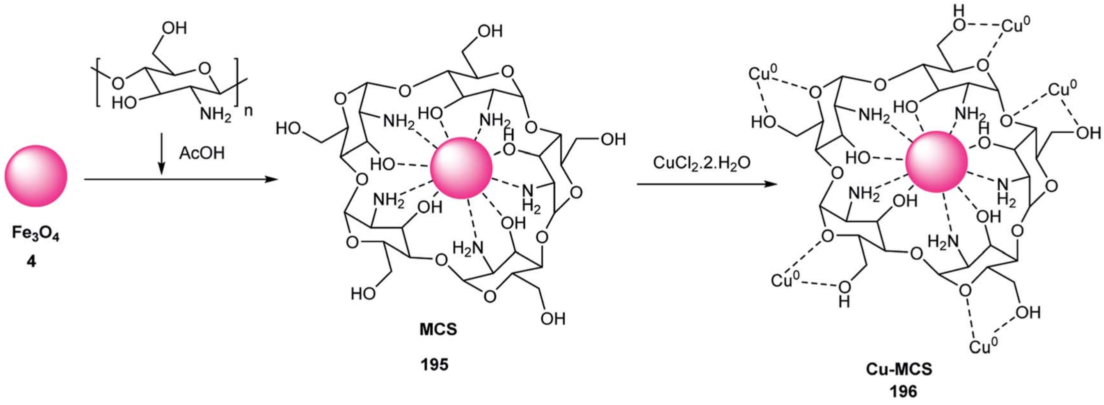

Scheme 67 Synthesis of Cu-MCS.

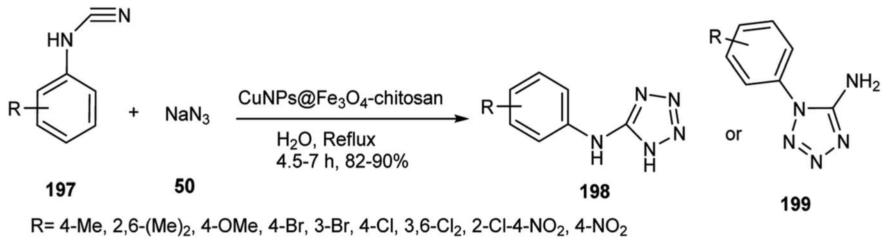

Scheme 68 Synthesis of various tetrazoles **198** or **199** using Cu-MCS.

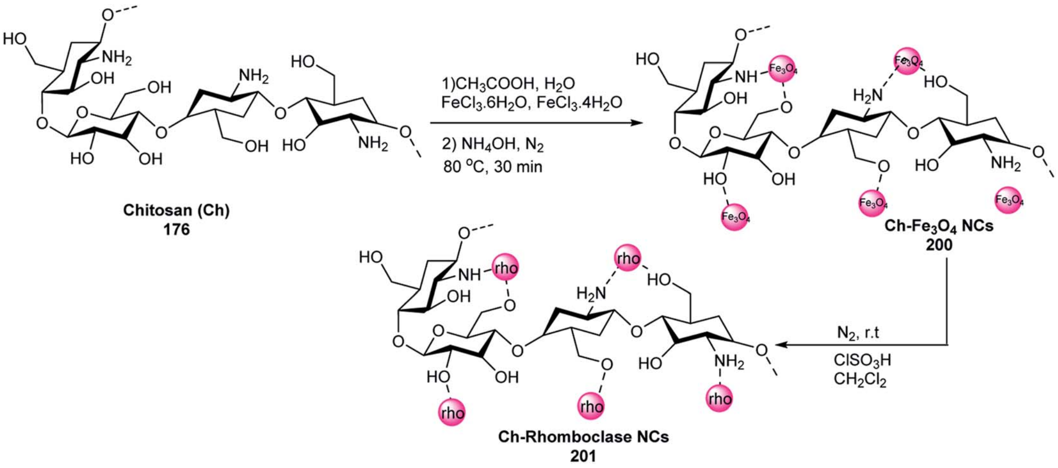

Scheme 69 Synthesis of Ch-rhomboclase NCs **201**.

and ethylenediamine were added to it. Then, this mixture was placed in a Teflon-lined autoclave and heated at 200 °C for 8 h to obtain Fe_3O_4/CS **205,** which was dispersed in DMSO under ultrasound irradiation to give CS-coated Fe_3O_4, followed by mixing with melamine **63** and terephthaldehyde **203**. The obtained mixture was transferred in a Teflon-lined autoclave at 180 °C for 12 h to obtain Fe_3O_4/CS/COF **206,** which was reacted with $Cu(NO_3)_2\cdot 3H_2O$ in EtOH under reflux conditions and argon atmosphere for 24 h to generate Fe_3O_4/CS/COF/Cu **207** (Scheme 71).[83]

The catalytic activity of Fe_3O_4/CS/COF/Cu **207** was tested in the synthesis of polyhydroquinolines **72** *via* the Hantzsch reaction of aldehydes **19**, dimedone **64**, ammonium acetate **71**, and ethyl acetoacetate **35** (Scheme 72). Fe_3O_4/CS/COF/Cu with two sites including a Lewis acid (Cu^{2+}) and Lewis base (imine) catalyzed the Hantzsch reaction, which was used five times without a decrease in its activity.[83]

Open Access Article. Published on 26 April 2022. Downloaded on 7/17/2025 7:12:56 PM. This article is licensed under a Creative Commons Attribution-NonCommercial 3.0 Unported Licence.

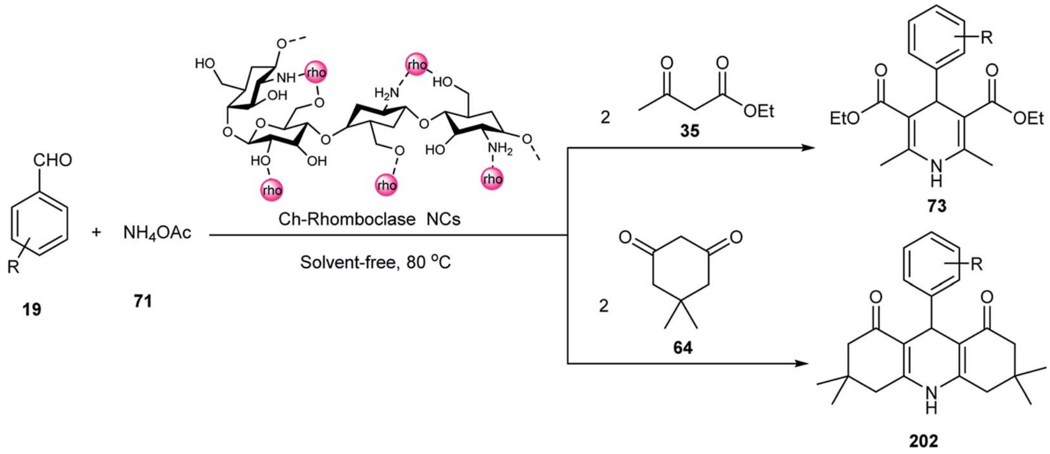

Scheme 70 Synthesis of 1,4-dihydropyridine derivatives **73** or **202**.

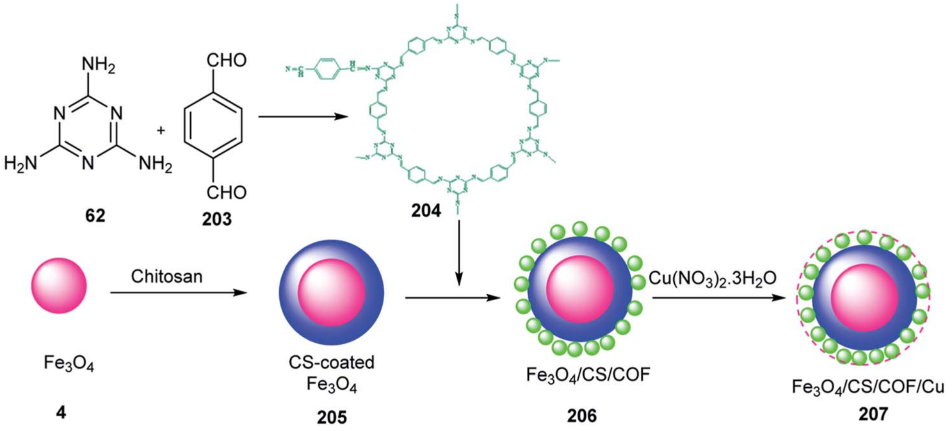

Scheme 71 Synthesis of the Fe_3O_4/CS/COF/Cu.

2.7. Synthesis and application of magnetic $ZnS/CuFe_2O_4$/agar

$FeCl_3\cdot6H_2O$ **1**, $CuCl_2\cdot2H_2O$ **208**, $Zn(OAc)_2.2H_2O$ **209**, and thioacetamide were dissolved in distilled H_2O. Then, agar **211** and ammonia solution were added to the reaction mixture to obtain $ZnS/CuFe_2O_4$/agar **212** (Scheme 73).[84]

The catalytic activity of $ZnS/CuFe_2O_4$/agar **212** was examined in the reaction of dimedone **64**, malononitrile **14**, and aldehydes **19** to synthesize 2-amino-tetrahydro-4*H*-chromene-3-carbonitriles **116** (Scheme 74). The carbonyl groups were activated in the presence of $ZnS/CuFe_2O_4$ *via* interaction with the hydroxyl groups of agar and Zn metal as a Lewis acid. The catalyst was reused five times with no reduction in its activity.[84]

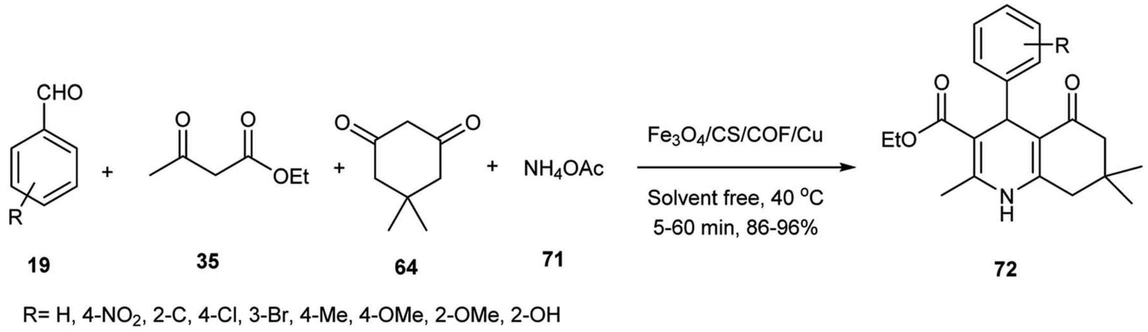

Scheme 72 Synthesis of polyhydroquinoline derivatives *via* Hantzsch reaction.

Open Access Article. Published on 26 April 2022. Downloaded on 7/17/2025 7:12:56 PM.
This article is licensed under a Creative Commons Attribution-NonCommercial 3.0 Unported Licence.

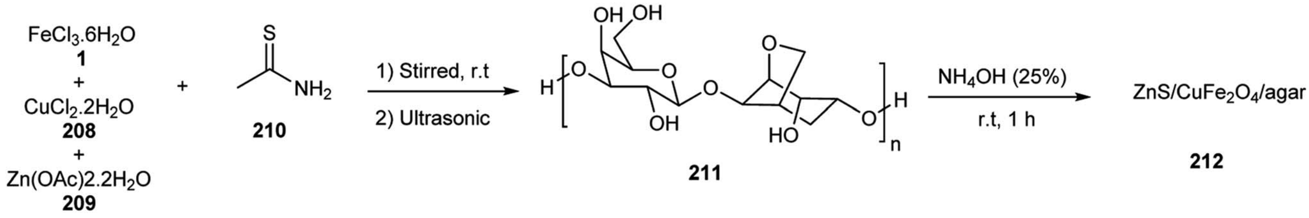

Scheme 73 Synthesis of ZnS/CuFe$_2$O$_4$/agar **212**.

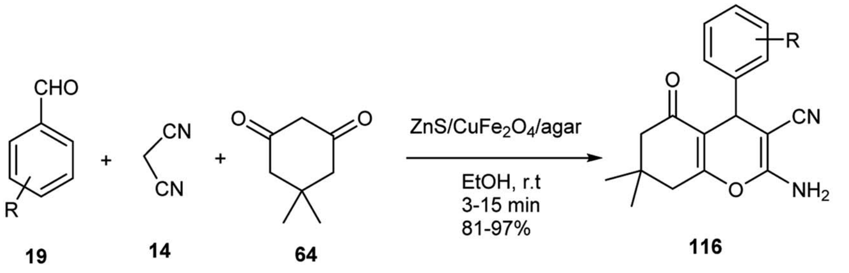

R= 4-NO$_2$, 3-NO$_2$, 2-Cl, 3-Cl, 4-Cl, 3-Me, 4-Me, 4-CH(Me)$_2$, 2-OMe, 3-OMe, 4-OMe, 3,4,5-(OMe)$_3$, 3-OH, 4-OH, 2,4-Cl$_2$

Scheme 74 Synthesis of 2-amino-tetrahydro-4*H*-chromene-3-carbonitrile derivatives.

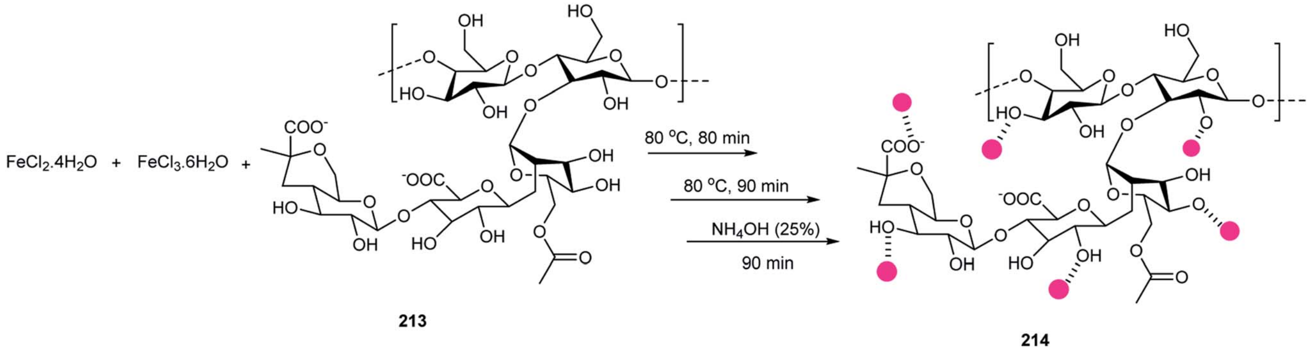

Scheme 75 Synthesis of Fe$_3$O$_4$@xanthan gum **214**.

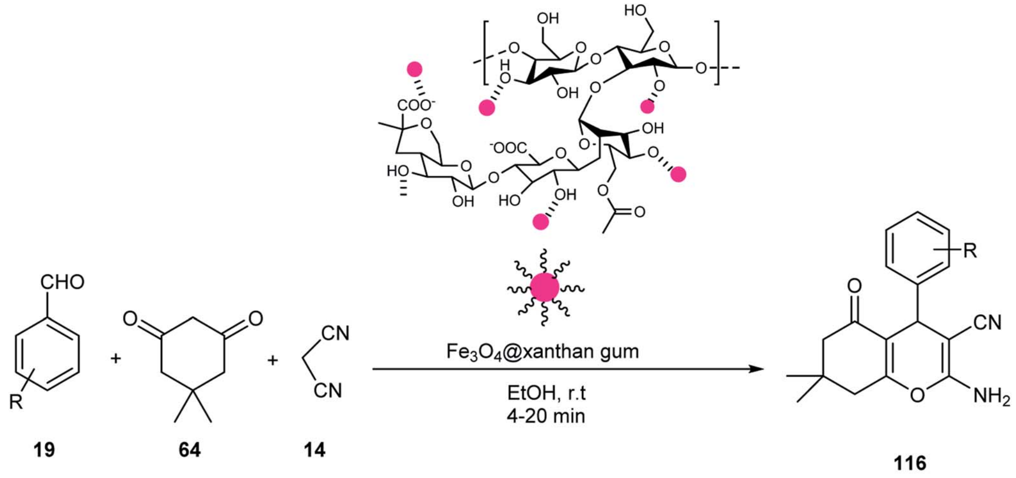

R= 2-Cl, 4-Cl, 2,4-Cl2, 2,6-Cl2, 2-Br, 4-CN, 3-Me

Scheme 76 Synthesis of 2-amino-3-cyano-4*H*-pyran derivatives **116** using Fe$_3$O$_4$@xanthan gum.

Open Access Article. Published on 26 April 2022. Downloaded on 7/17/2025 7:12:56 PM. This article is licensed under a Creative Commons Attribution-NonCommercial 3.0 Unported Licence.

2.8. Synthesis and application of magnetic Fe_3O_4@xanthan gum

NH_4OH solution was added to a mixture of the $FeCl_2 \cdot 4H_2O$, $FeCl_3 \cdot 6H_2O$ (1 : 2), and an aqueous suspension of xanthan gum **213** to give Fe_3O_4@xanthan gum **214** (Scheme 75).[85]

Fe_3O_4@xanthan gum was applied in the synthesis of 2-amino-3-cyano-4*H*-pyran derivatives **116** *via* the reaction of aldehydes **19**, dimedone **64**, and malononitrile **14** in EtOH (Scheme 76). The model reaction was performed about nine times and the yields did not decrease. This reaction was accomplished in the presence of Fe_3O_4 after 45 min in 30% yield. It was shown that Fe_3O_4@xanthan gum activated the carbonyl groups *via* hydrogen bonding, which was more effective than Fe_3O_4.[85]

3. Conclusion

Many bio-polymers can be obtained from natural sources. According to the importance of green chemistry in organic reactions, in this review, the application of bio-polymers as a catalyst in multicomponent reactions was grouped and summarized. Herein, we highlighted the immobilization of magnetic nanoparticles with bio-polymers. Due to the excellent properties of magnetic nano-catalysts, including their non-toxic nature, high surface area, simple preparation, easy surface modification, and simple separation, these systems have been applied as catalysts in multicomponent reactions. Various organic compounds such as bio-polymers were used for the modification of magnetic nanoparticles. Bio-polymers have various advantages such as biodegradable, biocompatible, and heat-resistant nature. Therefore, herein, their synthesis and catalytic activities in multicomponent reactions were studied. We believe that this article will guide researchers in the design and synthesis of various compounds according to green chemistry. Magnetic nanocomposites have many applications in various fields including, drug delivery, solar cells, chemical sensors, water treatment, biomedical sensors, and catalysts. The importance of these topics could be discussed as a review article in the future.

Conflicts of interest

There are no conflicts to declare.

Acknowledgements

We are grateful for the Research Council's support of Alzahra University.

References

1 A. Ali, H. Zafar, M. Zia, U. HAQ, A. Phull, J. Ali and A. Hussain, *Nanotechnol., Sci. Appl.*, 2016, **9**, 49–67.
2 F. Erogbogbo, K.-T. Yong, R. Hu, W.-C. Law, H. Ding, C.-W. Chang, P. N. Prasad and M. T. Swihart, *ACS Nano*, 2010, **4**, 5131–5138.
3 M. Esmaeilpour, J. Javidi, F. N. Dodeji and H. Hassannezhad, *J. Iran. Chem. Soc.*, 2014, **11**, 1703–1715.
4 L. Lai, Q. Xie, L. Chi, W. Gu and D. Wu, *J. Colloid Interface Sci.*, 2016, **465**, 76–82.
5 A. Abou-Hassan, O. Sandre, S. Neveu and V. Cabuil, *Angew. Chem.*, 2009, **121**, 2378–2381.
6 N. O. Mahmoodi, F. Ghanbari Pirbasti and Z. Jalalifard, *J. Chin. Chem. Soc.*, 2018, **65**, 383–394.
7 M. Esmaeilpour, J. Javidi and M. Zandi, *New J. Chem.*, 2015, **39**, 3388–3398.
8 X. Chen, Y. Zhou, H. Han, X. Wang, L. Zhou, Z. Yi and L. Zeng, *Mater. Today Chem.*, 2021, **22**, 100556.
9 G. U. I. Sheng, S. H. E. N. Xiaodong and L. I. N. Benlan, *Rare Met.*, 2006, **25**, 426–430.
10 S. S. Khasraghi, M. Shojaei, M. Janmaleki and U. Sundararaj, *Eur. Polym. J.*, 2021, **159**, 110735.
11 X. Liu, J. Tian, Y. Li, N. Sun, S. Mi, Y. Xie and Z. Chen, *J. Hazard. Mater.*, 2019, **373**, 397–407.
12 M. Muthiah, I. K. Park and C. S. Cho, *Biotechnol. Adv.*, 2013, **3**, 1224–1236.
13 R. Mohammadi, A. Saboury, S. Javanbakht, R. Foroutan and A. Shaabani, *Eur. Polym. J.*, 2021, **153**, 110500.
14 M. A. Almessiere, Y. Slimani, A. Demir Korkmaz, A. Baykal, H. Albetran, T. A. Saleh, M. Sertkol and I. Ercan, *Ultrason. Sonochem.*, 2020, **62**, 104847.
15 H. Javadian, M. Ruiz, T. A. Saleh and A. M. Sastre,*J. Mol. Liq.*, 2020, **306**, 112760.
16 A. A. Basaleh, M. H. Al-Malack and T. A. Saleh, *J. Environ. Chem. Eng.*, 2021, **9**, 105126.
17 A. A. Basaleh, M. H. Al-Malack and T. A. Saleh, *Sustainable Chem. Pharm.*, 2021, **23**, 100503.
18 N. Dhenadhayalan, K. C. Lin and T. A. Saleh, *Small*, 2020, **6**, 1905767.
19 A. M. Alansi, M. Al-Qunaibit, I. O. Alade, T. F. Qahtan and T. A. Saleh,*J. Mol. Liq.*, 2018, **253**, 297–304.
20 A. M. Alansi, T. F. Qahtan and T. A. Saleh, *Adv. Mater. Interfaces*, 2021, **8**, 2001463.
21 A. M. Alansi, T. F. Qahtan, N. Al Abass, J. M. AlGhamdi, M. Al-Qunaibit and T. A. Saleh, *Adv. Sustainable Syst.*, 2021, 2100267.
22 T. A. Saleh, *Environ. Technol. Innovation*, 2021, **24**, 101821.
23 J. Wang, Z. Shi, J. Fan, Y. Ge, J. Yin and G. Hu, *J. Mater. Chem.*, 2012, **22**, 22459.
24 T. A. Debele, S. L. Mekuria and H. C. Tsai, *Mater. Sci. Eng., C*, 2016, **68**, 964–981.
25 A. Maleki and M. Kamalzare, *Catal. Commun.*, 2014, **53**, 67–71.
26 V. Omid, F. M. Kievit, C. Fang, N. Mu, S. Jana, M. C. Leung, H. Mok, R. G. Ellenbogen, J. O. Park and M. Zhang, *Biomaterials*, 2010, **31**, 8032–8042.
27 Z. M. Avval, L. Malekpour, F. Raeisi, A. Babapoor, S. M. Mousavi, S. A. Hashemi and M. Salari, *Drug Metab. Rev.*, 2020, **52**, 157–184.
28 S. Mirza, M. S. Ahmad, M. I. A. Shah and M. Ateeq, In *Metal nanoparticles for drug delivery and diagnostic applications*, Elsevier, 2020, pp. 189–213.

© 2022 The Author(s). Published by the Royal Society of Chemistry

Open Access Article. Published on 26 April 2022. Downloaded on 7/17/2025 7:12:56 PM.
This article is licensed under a Creative Commons Attribution-NonCommercial 3.0 Unported Licence.

29 A. Gholami, S. M. Mousavi, S. A. Hashemi, Y. Ghasemi, W.-H. Chiang and N. Parvin, *Drug Metab. Rev.*, 2020, **52**, 205–224.

30 X. Sun, G. Zhang, R. Du, R. Xu, D. Zhu, J. Qian, G. Bai, C. Yang, Z. Zhang, X. Zhang and D. Zou, *Biomaterials*, 2019, **194**, 151–160.

31 Z. Zhou, L. Yang, J. Gao and X. Chen, *Adv. Mater.*, 2019, **31**, 1804567.

32 D. D. Stueber, J. Villanova, I. Aponte, Z. Xiao and V. L. Colvin, *Pharmaceutics*, 2021, **13**, 943.

33 N. M. El-Shafai, M. M. Abdelfatah, M. E. El-Khouly, I. M. El-Mehasseb, A. El-Shaer, M. S. Ramadan, M. S. Masoud and M. A. El-Kemary, *Appl. Surf. Sci.*, 2020, **506**, 144896.

34 L. Gloag, M. Mehdipour, D. Chen, R. D. Tilley and J. J. Gooding, *Adv. Mater.*, 2019, **31**, 1904385.

35 S. Khizar, H. Ben Halima, N. M. Ahmad, N. Zine, A. Errachid and A. Elaissari, *Electrophoresis*, 2020, **41**, 1206–1224.

36 M. P. Conte, J. K. Sahoo, Y. M. Abul-Haija, K. A. Lau and R. V. Ulijn, *ACS Appl. Mater. Interfaces*, 2018, **10**, 3069–3075.

37 S. Mallakpour and M. Hatami, *Appl. Clay Sci.*, 2019, **174**, 127–137.

38 N. Shabani, A. Javadi, H. Jafarizadeh-Malmiri, H. Mirzaei and J. Sadeghi, *Food Hyg.*, 2021, **10**, 61–71.

39 R. Banerjee, Y. Katsenovich, L. Lagos, M. McIintosh, X. Zhang and C.-Z. Li, *Curr. Med. Chem.*, 2010, **17**, 3120–3141.

40 S. Mallakpour, M. Tukhani and C. M. Hussain, *Int. J. Biol. Macromol.*, 2021, **179**, 429.

41 S. Kamel and T. A. Khattab, *Cellulose*, 2021, **28**, 4545.

42 G. Mohammadi Ziarani, Z. Kheilkordi, F. Mohajer, A. Badiei and R. Luque, *RSC Adv.*, 2021, **11**, 17456–17477.

43 G. Mohammadi Ziarani, S. Rohani, A. Ziarati and A. Badiei, *RSC Adv.*, 2018, **8**, 41048–41100.

44 F. Mohajer, G. Mohammadi Ziarani and A. Badiei, *RSC Adv.*, 2021, **11**, 6517–6525.

45 Z. Kheilkordi, G. Mohammadi Ziarani and F. Mohajer, *Curr. Org. Chem.*, 2022, **26**, 287–298.

46 G. Mohammadi Ziarani, R. Moradi, T. Ahmadi and N. Lashgari, *RSC Adv.*, 2018, **8**, 12069–12103.

47 G. Mohammadi Ziarani, F. Aleali and N. Lashgari, *RSC Adv.*, 2016, **6**, 50895–50922.

48 G. Mohammadi Ziarani, N. H. Nasab and N. Lashgari, *RSC Adv.*, 2016, **6**, 38827–38848.

49 L. A. Thompson, *Curr. Opin. Chem. Biol.*, 2000, **4**, 324–337.

50 A. Dömling, *Curr. Opin. Chem. Biol.*, 2002, **6**, 306–313.

51 E. Zare and Z. Rafiee, *Appl. Organomet. Chem.*, 2020, **34**, e5516.

52 S. S. Hosseinikhah and B. B. F. Mirjalili, *RSC Adv.*, 2020, **10**, 40508–40513.

53 P. G. Kargar, G. Bagherzade and H. Eshghi, *RSC Adv.*, 2020, **10**, 37086–37097.

54 A. Maleki, S. Gharibi, K. Valadi and R. Taheri-Ledari, *J. Phys. Chem. Solids*, 2020, **142**, 109443.

55 G. Bagherzade, *RSC Adv.*, 2021, **11**, 19203–19220.

56 G. Bagherzade and H. Eshghi, *RSC Adv.*, 2021, **11**, 4339–4355.

57 P. G. Kargar, M. Noorian, E. Chamani, G. Bagherzade and Z. Kiani, *RSC Adv.*, 2021, **11**, 17413–17430.

58 M. Zahedifar, B. Pouramiri and R. Razavi, *Res. Chem. Intermed.*, 2020, **46**, 2749–2765.

59 B. B. F. Mirjalili, Z. Zaghaghi and A. Monfared, *J. Chin. Chem. Soc.*, 2020, **67**, 197–201.

60 N. Safajoo, B. B. F. Mirjalili and A. Bamoniri, *Polycyclic Aromat. Compd.*, 2021, **41**, 1241–1248.

61 N. Safajoo, B. B. F. Mirjalili and A. Bamoniri, *RSC Adv.*, 2019, **9**, 1278–1283.

62 G. Bagherzade and H. Eshghi, *RSC Adv.*, 2020, **10**, 32927–32937.

63 A. D. Tafti and B. B. F. Mirjalili, *RSC Adv.*, 2020, **10**, 31874–31880.

64 A. Maleki, F. Hassanzadeh-Afruzi, Z. Varzi and M. S. Esmaeili, *Mater. Sci. Eng., C*, 2020, **109**, 110502.

65 Z. Amiri-Khamakani, F. Hassanzadeh-Afruzi and A. Maleki, *Chem. Process.*, 2020, **3**, 101.

66 E. Babaei and B. B. F. Mirjalili, *Iran. J. Catal.*, 2020, **10**, 219–226.

67 A. Mohammadzadeh, A. P. Marjani and A. Zamani, *S. Afr. J. Chem.*, 2020, **73**, 55–63.

68 M. Kamalzare, M. Bayat and A. Maleki, *R. Soc. Open Sci.*, 2020, **7**, 200385.

69 M. H. Sayahi, F. Shamkhani, M. Mahdavi and S. Bahadorikhalili, *Starch-Stärke*, 2021, **73**, 2000257.

70 S. Forouzandehdel, M. Meskini and M. R. Rami, *J. Mol. Struct.*, 2020, **1214**, 128142.

71 M. Shamsi-Sani, F. Shirini and M. Mohammadi-Zeydi, *J. Nanosci. Nanotechnol.*, 2019, **19**, 4503–4511.

72 S. Amirnejat, A. Nosrati and S. Javanshir, *Appl. Organomet. Chem.*, 2020, **34**, e5888.

73 S. Amirnejat, A. Nosrati, S. Javanshir and M. R. Naimi-Jamal, *Int. J. Biol. Macromol.*, 2020, **152**, 834–845.

74 M. Banazadeh, S. Amirnejat and S. Javanshir, *Front. Chem.*, 2020, **8**, 1023.

75 H. Ghavidel, B. Mirza and S. Soleimani-Amiri, *Polycycl. Aromat. Compd.*, 2021, **41**, 604–625.

76 S. Behrouz, M. N. Abi and M. A. Piltan, *Acta Chim. Slov.*, 2021, **68**, 374–386.

77 S. Behrouz, M. N. Abi and M. A. Piltan, *J. Appl. Chem.*, 2019, **14**, 109–124.

78 S. Asgharnasl, R. Eivazzadeh-Keihan, F. Radinekiyan and A. Maleki, *Int. J. Biol. Macromol.*, 2020, **144**, 29–46.

79 K. Javanmiri and R. Karimian, *Monatsh. Chem.*, 2020, **151**, 199–212.

80 H. Naeimi and S. Lahouti, *J. Org. Chem. Res.*, 2020, **6**, 54–68.

81 N. Motahharifar, M. Nasrollahzadeh, A. Taheri-Kafrani, R. S. Varma and M. Shokouhimehr, *Carbohydr. Polym.*, 2020, **232**, 115819.

82 P. Kamalzare, B. Mirza and S. Soleimani-Amiri, *J. Nanostructure Chem.*, 2021, **11**, 229–243.

83 E. Zare and Z. Rafiee, *J. Taiwan Inst. Chem. Eng.*, 2020, **116**, 205–214.

84 S. Bahrami, F. Hassanzadeh-Afruzi and A. Maleki, *Appl. Organomet. Chem.*, 2020, **34**, e5949.

85 M. S. Esmaeili, M. R. Khodabakhshi, A. Maleki and Z. Varzi, *Polycyclic Aromat. Compd.*, 2021, **41**, 1953–1971.